Activation of π-systems in Lewis acid mediated homogenous catalysis

Dissertation for the degree of Doctor Philosophiae

Mikko Muuronen
University of Helsinki
Faculty of Science
Department of Chemistry
Laboratory of Organic Chemistry
P.O. Box 55 (A.I. Virtasen aukio 1)
FI-00014 University of Helsinki, Finland

To be presented, with the permission of the Faculty of Science, University of Helsinki, for public discussion in Auditorium A129, Department of Chemistry (A.I. Virtasen aukio 1, Helsinki), on 22nd of May 2015, at noon.

Helsinki 2015

Supervised by

Dr. Juho Helaja
Department of Chemistry
University of Helsinki
Helsinki, Finland

Dr. Michael Patzschke
Department of Chemistry
University of Helsinki
Helsinki, Finland

Reviewed by

Prof. Ville Kaila
Department of Chemistry
Technical University of München
München, Germany

Dr. Heikki Tuononen
Department of Chemistry
University of Jyväskylä
Jyväskylä, Finland

Opponent

Prof. Robert Paton
Department of Chemistry
University of Oxford
Oxford, United Kingdom

ISBN 978-951-51-1167-8 (paperback)
ISBN 978-951-51-1168-5 (PDF)
http://ethesis.helsinki.fi
Unigrafia Helsinki 2015

I don't demand that a theory correspond to reality because I don't know what it is. Reality is not a quality you can test with litmus paper. All I'm concerned with is that the theory should predict the results of experiment.

— Stephen Hawking

Abstract

Understanding the electronic structure of a chemical system in detail is essential for describing its chemical reactivity. In the present work, quantum chemical methods are applied in combination with experimental studies to achieve such detailed mechanistic understanding of chemical systems. Understanding the basic theory behind computational methods is of importance when applying them to chemical problems. Therefore, the first part of this work provides an introduction to quantum chemical methods.

The results of this work are published in four peer-reviewed publications. In each publication, the understanding of the chemical system has been obtained using a combination of experimental and quantum chemical studies. These include the design of a new-type of Au(III)-catalysts, and understanding mechanistic aspects related to a Au(III) catalytic cycle. We have also focused on understanding how the electronic structure of an alkyne affects the regioselectivity in the Pauson-Khand reaction. A computational model, which provides a qualitative and, to some extent, a quantitative prediction of regiochemical outcomes is presented.

List of Publications

Publications representing the results of this work:

I. **M. Muuronen**, J.E. Perea-Buceta, M. Nieger, M. Patzschke and J. Helaja. Cationic Gold Catalysis with Pyridine-Tethered Au(III) NHC-Carbenes: An Experimental and DFT Computational Study. *Organometallics* **2012**, *31*, 4320-4330.

II. T. Wirtanen,† **M. Muuronen**,† M. Melchionna, M. Patzschke and J. Helaja. Gold(III) catalyzed enynamine - cyclopentadiene cycloisomerization with transfer of chirality: An experimental and theoretical study indicating involvement of dual Au(III) push-pull assisted *cis-trans* isomerism. *Journal of Organic Chemistry* **2014**, *79*, 10269-10283.

III. E. Fager-Jokela, **M. Muuronen**, M. Patzschke and J. Helaja. Electronic Regioselectivity of Diarylalkynes in Cobalt-Mediated Pauson Khand Reaction: An Experimental and Computational Study with Para- and Meta-Substituted Diarylalkynes and Norbornene. *Journal of Organic Chemistry* **2012**, *77*, 9134-9147.

IV. E. Fager-Jokela,† **M. Muuronen**,† H. Khaizourane,† A. Vázquez-Romero, X. Verdaguer, A. Riera and J. Helaja. Electronic regioguidance in Pauson-Khand reactions of aliphatically substituted alkynes by alkyne polarization via inductive effect. *Journal of Organic Chemistry* **2014**, *79*, 10999-11010.

† Shared first author.

List of other publications

V. V. Iashin, T.V. Koso, K. Stranius, **M. Muuronen**, S. Heikkinen, J. Kavakka, N. Tkachenko and J. Helaja. Chlorophyll tailored 20-trifluoroacetamide and its azacrown derivative as pH sensitive colorimetric sensor probe with response to AcO^-, F^- and CN^- ions. *RSC Advances* **2013**. *3*, 11485-11488.

VI. K. Stranius, V. Iashin, T. Nikkonen, **M. Muuronen**, J. Helaja and N. Tkachenko. Effect of Mutual Position of Electron Donor and Acceptor on Photoinduced Electron Transfer in Supramolecular Chlorophyll-fullerene Dyads. *Journal of Physical Chemistry A* **2014**, *118*, 1420-1429.

VII. O. Seppänen, **M. Muuronen** and J. Helaja. Gold catalyzed conversion of aryl and alkyl substituted aniline-2-propynones to corresponding 2-substituted 4-quinolones. *European Journal of Organic Chemistry* **2014**, *19*, 4044-4052.

VIII. T. Nikkonen, M. Moreno Oliva, A. Kahnt, **M. Muuronen**, J. Helaja and D.M. Guldi. Photoinduced charge transfer on self-assembling chlorin dimer-azafulleroid in polar and nonpolar media. *Chemistry - A European Journal* **2015**, *21*, 590-600.

Author contributions

The contributions of the authors in articles I-IV:

I. The author performed all experimental and computational work. JPB assisted with the research and MN performed the X-ray analysis. MP and JH supervised the work. The author drafted the manuscript, and the final version was modified and approved by all authors.

II. The work was divided equally between the author and TW (shared first authorship), for computational and experimental work, respectively. MP and JH supervised the work. The reaction mechanism was discussed and concluded with the efforts of all authors, and the author drafted the mechanistic studies. All authors edited and approved the final version.

III. The work was divided between the author and EF, for computational and experimental work, respectively. MP and JH supervised the work. The experimental results were drafted by EF, and the computational studies by the author. The final version of the manuscript was discussed and approved by all authors.

IV. The author planned and performed all computational work (shared first authorship). The experimental work was done by EF and HK and the work was supervised by JH and AR. Theoretical considerations were drafted mainly by the author. All authors discussed and approved the final version.

Acknowledgements

To start with, I want to express my gratitude to my two supervisors, Dr. Juho Helaja and Dr. Michael Patzschke, without whom this work would not have been possible. Juho, I joined your group to perform organometallic synthesis; but eventually I ended up on the computational side. I am deeply grateful to you for being constantly available for scientific discussions and for providing me with your full support with my choices. Michael, at the beginning of this work I came to your door to ask questions about quantum chemistry. During the time our collaboration evolved and you became my second supervisor. I owe my gratitude to both of you for sharing your knowledge and enthusiasm in chemistry with me. Thank you.

I am grateful to the reviewers of this thesis, Prof. Ville Kaila and Dr. Heikki Tuononen, for their careful reviews and the valuable feedback and suggestions which they provided. I want to acknowledge Prof. Robert Paton for being the opponent during the defense of this dissertation. I also want to thank Prof. Mikko Oivanen for his valuable suggestions and discussions, and for acting as the custos of the defense.

I have shared my publications with several co-authors, and I am grateful to all of them for their contributions and sharing their knowledge with me. I also want to thank Prof. Markku Räsänen, the Head of the Department of Chemistry, and Prof. Ilkka Kilpeläinen, the Head of the Laboratory of Organic Chemistry, for useful discussions and for allowing me the opportunity to work in such excellent research facilities.

I have also had the pleasure to visit Dr. Markus Pernpointner at the University of Heidelberg, and Prof. Feliu Maseras at the Institute of Chemical Research, Catalonia. I would like to express my deepest gratitude to both of you. I learned a lot during these visits and these have been unforgettable experiences for me. In Heidelberg, the theoretical chemistry group was like a big family and I want to thank you all for including me in it. I also really enjoyed myself in Tarragona, and I want to thank everyone in the computational chemistry group for that. I also want to thank Prof. Antoni Riera and his group for collaboration and hospitality during my visit to Barcelona.

This work would have never been possible without great support from all the past and present Helaja group members I have worked or shared the office

with: Erika, Taru, Tom, Aleksandar, Vladimir, Otto, Mikko, Jesus, Otto-Ville, Andy, Florian and Santeri. Thank you all for your collaboration and friendship. Tom, I want to thank you especially for your friendship and intensive collaboration during these years. Nothing can beat the golden times in our tea club! Erika, I always loved working and co-authoring with you, and Taru, your cheerful attitude and our scientific conversations have always been a delight.

During the years, I have had the pleasure to interact with many people in the department. I want to especially thank Prof. Pekka Pyykkö for sharing his knowledge in theoretical chemistry with me and assisting me with my future career. I am grateful to everyone in the laboratory of Organic Chemistry for all the help and companionship. I especially want to thank Dr. Jussi Sipilä, Dr. Sami Heikkinen, Dr. Petri Heinonen and Paula Nousiainen. I have also made many friends outside the group, and I want to thank especially Dr. Sergio Losilla, Antti Lahdenperä, Markus Lindqvist, Calle Suomivuori and Tuomas Kulomaa for numerous discussions and for their friendship. I want to acknowledge Professors Dage Sundholm, Timo Repo and Kristiina Wähälä for helpful discussions.

I have also had the pleasure of interacting with many scientists at conferences and in schools. I would especially like to thank Professors Filipp Furche and Anna Krylov for discussions, and Prof. Abhik Ghosh also for his friendship. I want to also express my gratitude to all attendees and lecturers of the ESQC 2013. I'll never forget the great people I met there, and in particular I want to thank Rebecca Sure for numerous helpful discussions.

Regarding funding, I want to acknowledge the University of Helsinki; the Emil Aaltonen and Gustaf Komppa Foundations; and the HPC-Europa2–program. Computational resources were provided by the Finnish Centre for Scientific Computing (CSC). Technical support by Dr. Nino Runeberg (CSC) is greatly acknowledged.

Finally, I want to express my deepest gratitude to my family. Mom, dad and my brother Antti, you have always been there for me, and this thesis would not be as it is without your endless support.

Mikko Muuronen
Helsinki, 2015

Contents

Abstract i

List of Publications ii

Acknowledgements v

List of Abbreviations ix

1 Introduction 1

2 Theoretical background 3

2.1 Common terminology 4

2.2 Approximations to the Molecular Hamiltonian 5

2.3 The Hartree-Fock method 6

2.3.1 Chemical perspective 7

2.3.2 Choice of the wave function 8

2.3.3 Other aspects 9

2.4 Electron correlation 10

2.4.1 Dynamic Correlation 11

2.4.2 Static Correlation 15

2.4.3 Need for static correlation? 17

2.5 Density functional theory 22

2.5.1 DFT functionals 23

2.5.2 DFT-D3 24

2.5.3 Self-interaction error 25

2.5.4 Accuracy of DFT 27

2.6 Relativistic effects 28

2.7 Basis set 29

2.7.1 Basis functions 29

2.7.2 Basis set families 30

2.8 Solvent effects 31

2.9 Transition State Theory 32

2.10 Molecular properties 34
2.10.1 Partial charges 34
2.10.2 NMR chemical shifts 35

3 Results **37**
3.1 Benchmark study for gold complexes 37
3.2 Development of the Au(III) catalyst 40
3.2.1 Further studies 43
3.3 Au(III) - Aspects of the reaction mechanism 45
3.4 Regioselectivity in the Pauson-Khand reaction 46
3.4.1 The reaction mechanism 47
3.4.2 Factors determining regioselectivity 48
3.4.3 Alkyne polarization 49
3.4.4 Weak interactions 51
3.4.5 Computational methods and accuracy 52

4 Conclusions **53**

Bibliography **55**

Appendix **77**

List of Abbreviations

BDE	Bond dissociation energy
BO	Born-Oppenheimer
CASSCF	Complete active space self-consistent field
CC	Coupled Cluster; truncated excitations are denoted with subfix S,D,T, etc.
CI	Configuration Interaction; truncated excitations are denoted with subfix S,D,T, etc.
COSMO	Conductor-like screening model
COSMO-RS	COSMO for real solvents
DCM	Dichloromethane
DFA	Density functional approximation
DFT	Density functional theory
DHF	Double hybrid functional
EDG	Electron donating group
EWG	Electron withdrawing group
GGA	Generalized gradient approximation
GIAO	Gauge-including atomic orbitals
GTO	Gaussian-type orbital
HF	Hartree-Fock
HOMO	Highest occupied molecular orbital
IGLO	Individual gauge for localized orbitals
KS-DFT	Kohn-Sham DFT
LDA	Local density approximation
LUMO	Lowest unoccupied molecular orbital
MAD	Mean absolute deviation
MeCN	Acetonitrile
MO	Molecular orbital
MP2	Second-order Møller-Plesset perturbation theory
NBO	Natural bonding orbital charges
NEVPT2	N-electron valence state perturbation theory
NHC	N-heterocyclic carbene
NMR	Nuclear magnetic resonance

PES	Potential energy surface
PK	Pauson-Khand
RECP	Relativistic effective core potential
RHF	Restricted Hartree-Fock
RI	Resolution of identity
ROHF	Restricted-open-shell Hartree-Fock
SCF	Self-consistent field
SCS-MP2	Spin-component-scaled MP2
SIE	Self-interaction error
SOC	Spin-orbit coupling
SOMO	Singly occupied molecular orbital
SR	Scalar relativistic
STO	Slater-type orbital
TFE	Trifluoroethanol
TM	Transition metal
TON	Turnover number
TS	Transition state
TST	Transition state theory
UHF	Unrestricted Hartree-Fock
WFT	Wave function theory
ZORA	Zeroth-order regular relativistic approximation

1 Introduction

One of the greatest challenges for quantum chemistry is not only to rationalize experimental results or phenomena, but also to predict the outcome of experiments. Ideally, a huge amount of experimental work could be replaced by simulation, thereby providing a cost-efficient and also industrially feasible alternative for reaction and catalyst design. This is unfortunately very complicated and, in the author's experience, computational prediction in catalyst design is rarely achieved without a strong experimental collaboration. While experimental development may proceed by itself, it can benefit significantly from computational studies when both fields collaborate towards understanding the chemistry of the system under study (Fig. 1.1).

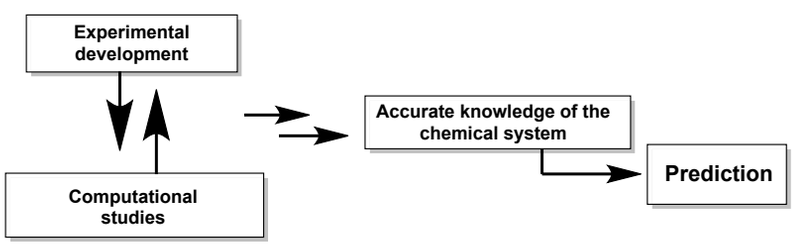

Fig. 1.1 Author's view of efficient computational prediction of chemical reactivity and properties.

During the past decade, the potential of quantum chemistry has been widely recognized in the experimental community and currently it is very common to find a section covering computational aspects in many experimental research articles. Rapid development of computers and new, more efficient algorithms allow experimental chemists to perform their own computations using even normal desktop computers. While the resources allow this, one must still keep in mind that computational chemistry is not a black box where the results are obtained by pressing a button. The experimental understanding of chemistry is simply not enough; insight into theoretical methods is also required to obtain trustworthy information. At its best, quantum chemistry is a powerful tool for rationalizing [1] or sometimes rejecting [2] experimental results, and

can also be used to successfully predict new molecules. [3, 4]

This thesis is written with the intention that it may serve as a guide for chemists to gain an overview of quantum chemical methods which may be used to solve problems related to organic and organometallic chemistry in electronic ground state. For readers looking for a deeper insight, [5–9] or a gentler introduction to the topic, [10] a number of good text books are available.

Quantum chemical methods have been applied in this work to understand the catalytic properties of Au(III) complexes and the factors affecting the regioselectivity in the Pauson-Khand reaction. The outcome of each study has been influenced and guided by experiments. A summary of the results is described in Chapter 3.

2 Theoretical background

Chemists have interest in computational quantum chemistry because it allows to compute specific properties of the system from the wave function Ψ. The wave function which, in principle, includes all information about the physical system in the non-relativistic limit, can be obtained by solving the following time-independent Schrödinger equation:

$$\hat{H}\Psi(R,r) = E\Psi(R,r), \tag{2.1}$$

where $\hat{H}$ is a Hamiltonian operator that describes the potential and kinetic energy of the system, $\Psi(R,r)$ is a wave function depending on the position of all nuclei (R) and electrons (r), and E is the total energy of the system with wave function $\Psi(R,r)$.

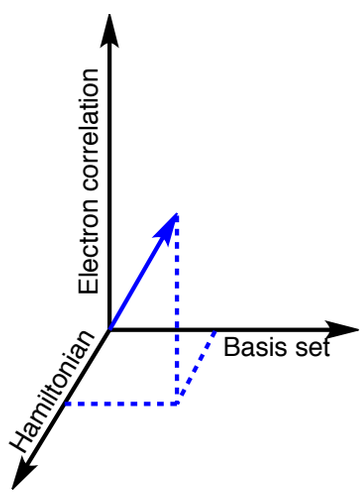

Fig. 2.1 The accuracy of the computational result is dependent on the Hamiltonian, treatment of electron correlation and the basis set used.

The Equation 2.1 can only be solved exactly for one electron-systems, but for studying larger molecules, one needs to introduce approximations in the Hamiltonian, electron correlation and basis set (Fig. 2.1). Approximations

define the limiting accuracy of each axis and therefore to obtain an accurate result, all three need to be solved accurately. Each one is highly important, as $\hat{H}$ includes the physical treatment of the system; electron correlation determines how electrons interact with each other; and the basis set determines the flexibility of the solution.

Quantum chemical methods can be divided into two separate categories, discussed here as methods based on wave function theory (WFT) or density functional theory (DFT). Both theories are *ab initio* in the sense that the properties of the system may be solved from first principles without the need for empirical data. In this chapter, the theoretical basis for the general approximations applied in this work to treat problems related to organic and organometallic chemistry computationally is presented.

2.1 Common terminology

To clarify the subsequent discussion, terms which will be often mentioned, such as 'variational principle', 'size consistency', 'scaling' and 'RI-approximation' are explained here. [5, 6]

- According to the variational principle, the expectation value of the energy in Equation 2.1 evaluated using an approximate ground state wave function is always higher than the true energy of the system. Methods for generating approximate wave functions that utilize this principle are called variational and the best possible wave function is obtained by minimizing the energy.

- Another important term is size consistency. [11] This can be understood by a simple example which considers the energy of a system that is constructed from two subsystems, $\mathbf{A} + \mathbf{A}$. When the two subsystems do not interact, the energy of the studied system $\mathbf{A} + \mathbf{A}$ should be equal to $2\mathbf{A}$. Methods that satisfy this statement are called size consistent. While this might seem self-evident, there are a number of electronic structure methods that are size inconsistent. The origin of the size inconsistency is explained later (2.4.1.5).

- Different computational methods have different costs. The computational time is not discussed as any finite time but as scaling. Scaling is determined as a prefactor N^n where N is the size of the system and n the scaling factor, specific for each method. The size of the system is defined by the number of basis functions, which is dependent on the number of the electrons in the system as well as the size of basis set as explained in 2.7.

- The resolution of identity (RI) approximation is frequently used in this work. The benefit of the approximation is that it reduces the computational cost significantly without a significant loss in the accuracy. Multiple variants with different acronyms exist, e.g. RI, RI-JK and RIJ-COSX. [12–18] In these approximations, some of the necessary integrals are fitted in an auxiliary basis set. From a practical point of view, this means that the auxiliary basis set also needs to chosen, which is as important as the conventional basis set.

2.2 Approximations to the Molecular Hamiltonian

To solve problems related to organic and organometallic chemistry computationally, one usually makes two general assumptions to generate an approximate Hamiltonian. First, relativistic effects, which are described in 2.6, are neglected as they are not considered to be important for light main group elements. [19, 20] The exact non-relativistic time-independent equation is called the Schrödinger equation. When neglecting only the relativistic treatment from the Hamiltonian operator $\hat{H}$, a non-relativistic exact Hamiltonian can be presented as:

$$\hat{H} = \hat{T}_N + \hat{T}_e + \hat{V}_{Ne} + \hat{V}_{ee} + \hat{V}_{NN}. \tag{2.2}$$

Two first terms, $\hat{T}_N$ and $\hat{T}_e$, correspond to the kinetic energy operators of nuclei N and electrons e. The rest of the terms describe the potential energy of the system: Term $\hat{V}_{Ne}$ describes how nuclei N interact with electrons e, whereas terms $\hat{V}_{ee}$ and $\hat{V}_{NN}$ describe how electrons or nuclei interact with other electrons (ee) or nuclei (NN), respectively.

A second common approximation is the Born-Oppenheimer (BO) approximation, [21] which assumes that the electronic motion can be solved while keeping the nuclear positions fixed. This is justified because light electrons move significantly faster than heavier nuclei and instantaneously respond to any changes in the relative position of the nuclei.

As a consequence, the Hamiltonian can be separated into its electronic and nuclear parts, where the electronic part can be solved separately while keeping the position of the nuclei fixed:

$$\hat{H} = \hat{H}_{\text{nuc}} + \hat{H}_{\text{el}}. \tag{2.3}$$

Because the nuclei are considered to be static, their kinetic energy operator is neglected from the Equation 2.2. The nuclear repulsion term $\hat{V}_{NN}$ is not dependent on electronic coordinates but is constant for each specific nuclear

geometry. The full non-relativistic BO electronic Hamiltonian can be written:

$$\hat{H}_{BO} = \hat{H}_{\text{el}} + \hat{V}_{NN} = \hat{T}_e + \hat{V}_{Ne} + \hat{V}_{ee} + \hat{V}_{NN}. \tag{2.4}$$

If these were the only approximation involved in solving Equation 2.1, the obtained wave function would be exact in the limits of non-relativistic and BO approximations. However, solving the equation exactly for many-electron systems is still impossible, so further approximations are introduced: simplified treatments of electron correlation and finite basis sets.

The reader should also be aware that the BO-approximation may break down in chemical systems. The problem arises when two or more BO potential energy surfaces (PES) are separated by an energy which is of the same order of magnitude as the energy of nuclear motion. For example, this may occur in metal surfaces [22] or even in graphene [23], where the energy gap between the ground state and the excited state is small. Photochemical reactions may also be problematic due to the coupling of more than one BO PES. [24, 25]

2.3 The Hartree-Fock method

To obtain approximate solutions to the BO electronic hamiltonian, the Hartree-Fock (HF) method may be used. This is based on the one-particle approximation, where the wave function is built from products of single electron wave functions called spin orbitals. [26, 27] To satisfy the Pauli exclusion principle, the wave function is represented as a single Slater determinant of these spin orbitals. [28]

The formed Slater determinant would be an exact solution of the Hartree-Fock Hamiltonian in the limit of an infinite basis set; but as the wave function is constructed from spin orbitals depending on one electron, only electrons with the same spin can interact with each other through the Slater determinant. This does not affect the one-electron terms $\hat{T}_e$ and $\hat{V}_{Ne}$ in the electronic Hamiltonian but, the electron-electron repulsion term $\hat{V}_{ee}$ is, however, dependent on the coordinates of two electrons.

To account for the electron-electron repulsion, $\hat{V}_{ee}$ is replaced by an effective field $\hat{V}_{ee}^{eff}$ which describes the average effect of all electrons. This is why the Hartree-Fock method is also called the mean field approximation. The field is dependent on the position of all electrons and is solved iteratively until a self-consistent field (SCF) solution is obtained. The effective field describes the position of all electrons, and therefore, each electron (incorrectly) interacts also with itself. However, this self-interaction error (SIE) is cancelled exactly with the electron exchange energy when solving the Hartree-Fock-Roothan

equations. As the HF method is variational, the best ground state SCF solution is found by minimizing the energy.

The HF method recovers 99% of the electronic energy of the system in most cases. The missing 1% relates to the ability of an electron to respond rapidly to the movement of other electrons, a phenomena that is called electron correlation. [6] It should be emphasized that the total electronic energy is a large quantity, and a reaction barrier of e.g. 20 kcal/mol is only a small fraction even from the missing 1%.

2.3.1 Chemical perspective

The missing 1% being neglected in the HF method has a significant impact on chemistry. First, the electrons are too close to each other, because they are described by their average position and are not allowed to respond to the rapid movement of nearby electrons. As a consequence, the predicted bond lengths are in general too short. This causes overestimation of activation energies and vibrational frequencies. [6]

Second, some weak interactions such as dispersion forces are completely absent in the HF method, and these are often of importance in describing e.g. enantioselective catalysis correctly. [29, 30] The electron clouds of non-bonded fragments may interact with each other repulsively or attractively, depending on the distance separating them. In the HF method, electrons are aware of the average position of other electrons, and therefore the repulsive effect is taken into account trough the SCF procedure.

The attractive effect is easy to understand when considering a polarized molecule where the electrons are distributed unevenly, producing a permanent dipole moment. When two such systems interact together, the positive side of both fragments feels attraction to the negatively polarized side of the other fragment. These are called dipole-dipole interactions and hydrogen bonding belongs to this class. Weak interactions that rise from permanent dipole moments are described at the HF level. [6]

However, electron correlation is essential to describe the attractive dispersion forces, such as aromatic π-π -stacking between two benzene molecules. Due to the rapid movement of electrons, each molecule has always a small non-permanent and rapidly changing dipole moment. This non-permanent dipole moment is capable of polarizing the other fragment, creating an attraction. By neglecting the ability of electrons to respond to the rapid movement of other electrons, the HF method completely neglects these so-called dispersion interactions. [6]

The inclusion of dispersion forces is not only necessary to describe non-bonded systems, but also affects the stability of molecules. For instance, the

stability of branched alkanes over linear chain isomers is due to electron correlation [31–35] and even the existence of some molecules might be dependent on it. [36] Therefore reactions where the electron correlation of the system changes in the course of the reaction are problematic for the HF method, because by neglecting electron correlation, it does not treat the reactants and products equivalently. Some examples are alkane isomerization reactions and computation of bond dissociation energies (BDE). [5] Therefore it is easy to understand why substantial efforts are made to account for electron correlation, as described later.

2.3.2 Choice of the wave function

Before starting a HF computation, one has to specify how the method treats the spin-orbitals. This is done by choosing the type of wave function. In the restricted Hartree-Fock (RHF) method, the α and β spin-orbitals are treated in pairs, and the system is forced to have each orbital either doubly occupied or unoccupied. If this restriction is removed, and the α and β spin-orbitals are treated independently, the method is called the unrestricted Hartree-Fock (UHF). The restricted-open-shell Hartree-Fock (ROHF) method is a combination of these two, where unpaired electrons are treated as UHF and doubly occupied as RHF.

The restriction in the RHF method has a major drawback, which can be understood by considering the RHF wave function for H_2. The wave function is a product of single electron wave functions $\Psi = \varphi(1)\varphi(2)$, where $\varphi(1)$ and $\varphi(2)$ include the coordinates of electrons 1 and 2, respectively. In the equilibrium structure, both electrons occupy the lowest energy orbital that is formed as a combination of $1s$ orbitals of both hydrogens A and B:

$$\varphi_1 = \varphi_2 = 1s_A + 1s_B \tag{2.5}$$

Since, the hydrogens are identical, the wave function can be presented as:

$$\Psi = \varphi(1)\varphi(2) = (1s_A 1s_A) + (1s_A 1s_B) + (1s_B 1s_A) + (1s_B 1s_B). \tag{2.6}$$

This means that 50% of the wave function has ionic character with both electrons centered on the same nucleus (the first and the last terms); and 50% has covalent character with the electrons shared between the nuclei (the middle terms). Therefore the RHF method predicts covalent bonds to be too ionic and overestimates dipole moments. [6] The effect is most significant when considering the dissociation of the H_2 molecule. In the gas-phase, the

dissociation should be purely homolytic, whereas the RHF method considers the dissociation to be 50% heterolytic and 50% homolytic. [8]

To correct the dissociation behavior, the α- and β-spin-orbitals are treated independently in the UHF method and the method is more flexible. Unfortunately the UHF wave function suffers from spin-contamination, which is a disadvantage. This is a computational artifact, caused by mixing higher spin states with the singlet wave function. [6] In this example, the wave function of the dissociated hydrogen would be a combination of the singlet and the triplet states (see example in 2.4.3.1).

In addition to the UHF method, the dissociation behaviour of the RHF method can be corrected with electron correlation as discussed *vide infra*. When using the UHF method, the expectation value $\hat{S}^2$ of the wave function should be checked carefully to correspond to the correct spin state. Three common $\hat{S}^2$ values for organic chemists are shown in Table 2.1, defined as $S(S+1)$ where S is the total spin of the system.

Table 2.1 Expectation values $\hat{S}^2$ for three common spin states.

Spin-state	S	$\hat{S}^2$
singlet	0	0
doublet	1/2	0.75
triplet	1	2

2.3.3 Other aspects

The use of the 'pure' Hartree-Fock method in chemical applications is now mostly of historical interest. It is not very accurate, as was pointed out, and the lack of electron correlation is a serious disadvantage when describing chemical reactions. The Hartree-Fock method should not be, however, underestimated. It is the cheapest wave function based *ab initio* method, scaling as N^4; and most importantly, it forms the basis for both more accurate and more approximate methods. The accuracy is improved systematically by increasing the amount of electron correlation, whereas semi-empirical methods are formed by introducing more approximations. [37] The HF method is also size consistent.

Grimme and coworkers [38] showed recently that the HF model can be greatly improved to treat dispersion interactions with a separately defined energy correction based on DFT-D3 (2.5.2). Sure and Grimme also reported a fast and parameterized version of the HF method called HF-3c [39] which might have a significant potential, especially for preliminary optimizations of large supramolecular complexes. [40]

2.4 Electron correlation

To improve the HF result systematically, electron correlation is needed. Electron correlation is defined as the energy difference between the exact and the HF solution (with the same Hamiltonian and basis set):

$$E_{\mathrm{Corr}} = E_{\mathrm{Exact}} - E_{\mathrm{HF}}. \tag{2.7}$$

The Hartree-Fock solution is based on only one determinant of spin orbitals, and it should be the best single determinant solution that can be obtained. To allow an electron to respond rapidly to the movement of another electron, a simple way is to construct the wave function using more Slater determinants:

$$\Psi = a_0\phi_{\mathrm{HF}} + \sum_i a_i\phi_i, \tag{2.8}$$

where a_i is a coefficient, and ϕ_i is a Slater determinant with a specific electron configuration. The value of a_0 is usually close to 1 as the HF solution is the most stable single determinant solution: After all, it captures 99% of the total energy. The different electron configurations are obtained by moving electrons from occupied orbitals to unoccupied orbitals. These are called *excitations* and the total spin of the system does not change during them. The excitations are termed as single (S), double (D), triple (T) etc. depending on how many electrons are excited in all possible combinations. Examples of single and double excitations are shown in Fig. 2.2.

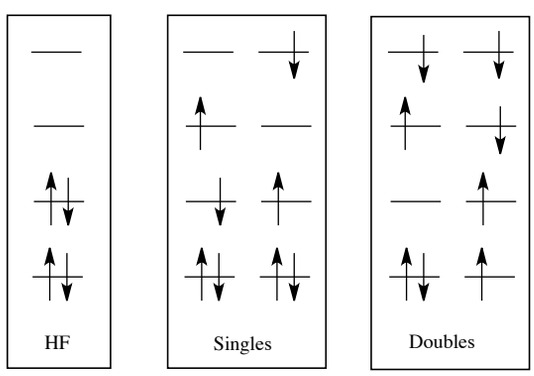

Fig. 2.2 Examples of single and double excitations of the HF solution.

This new, more flexible wave function is then optimized with respect to the total energy. The new energy obtained is lower than the Hartree-Fock energy by an amount which is an estimate of the electron correlation energy of the system. If all possible excitations for all electrons are taken into account, the obtained electron correlation would be exact in the given basis set. However,

the amount of required excitations rises factorially with increasing system size and therefore the types of excitations are commonly truncated e.g. to include only single and double excitations.

Computing the electron correlation energy in the WFT methods is based on these excitations. There are several ways to compute it, and the methods differ mainly on how the coefficients are determined in the Equation 2.8. The WFT methods used to treat static and dynamic electron correlation in this work are described. These two correlation effects have different chemical origins, which are explained below, but it is not always possible to make a clear distinction between them. However, understanding the main element is important in order to choose the optimal method for the problem.

2.4.1 Dynamic Correlation

Dynamic correlation is a short range correlation effect and the aim is to account for the missing 1% of the electronic energy by allowing the electrons to respond rapidly to the movement of the others. [5, 6, 8] It is based on the assumption that the HF molecular orbitals are qualitatively correct. In order to facilitate the computation, the orbitals are not re-optimized during the excitations.

2.4.1.1 Configuration interaction

The simplest way to account for dynamic correlation is to use the so-called Configuration Interaction (CI) method. Different electron configurations are formed in excitations, and the coefficients in Equation 2.8 are optimized in order to obtain the weights of these configurations. In the full CI method, all possible excitations are taken into account and the obtained solution is exact within the limits of the Hamiltonian and basis set. Performing such computations for large molecules is not computationally efficient as the amount of excitations rises factorially with the system size. The full CI method is typically used for small systems to benchmark other less accurate methods for electron correlation. [41–44]

A common practice is to truncate the expansion at some finite order. According to Brillouin's theorem, the singly excited states do not improve the HF ground state energy, [45] and the major contribution to the ground state energy comes typically from the double excitations. If only double excitations are taken into account, the method is called CID. Although the singly excited states do not mix directly with the HF solution, they allow the HF orbitals to relax. The computational cost does not increase much if they are added, and therefore the CISD method, taking into account also the single excitations, is a typical truncated version of the CI. While the full CI is variational and size

consistent, truncated versions of CI are not size consistent. [6]

2.4.1.2 Perturbation Theory

The basis of perturbation theory is that the HF solution is close to the desired exact solution and therefore the solution can be improved by adding electron correlation as a small perturbation. This leads to following ansatz of Equation 2.1:

$$\hat{H}\Psi = (\hat{H}_0 + \lambda\hat{H}^{'})\Psi = E\Psi, \tag{2.9}$$

where $\hat{H}_0$ is the unperturbed Hamiltonian and $\lambda\hat{H}^{'}$ is the perturbation that represents the difference between $\hat{H}_0$ and the exact Hamiltonian. The parameter λ ranges from zero to one, representing the extremes of the unperturbed and fully perturbed system, respectively.

By generating different excitations as described above, the $\lambda\hat{H}^{'}$ is applied to describe the electron correlation. The first order correction is already included in the HF energy, and therefore the second order correction is needed to improve the result. The most common method based on this is the second order Møller-Plesset perturbation theory (MP2) involving only double excitations. [46, 47] Higher order corrections can also be added: MP4 includes also triple and quadruple excitations but, unlike in the CI method, the quality of the solution is not necessarily improved by adding higher order corrections. [48] MP methods are size-consistent but not variational.

Among the WFT methods, the MP2 method is computationally the most efficient for describing dynamic electron correlation contribution to the energy and it can be also applied to large systems. It captures usually 80 - 90% of the electron correlation [6] and is not much more expensive than the HF method. It scales formally as N^5 but a major speed-up is obtained with the use of the RI-approximation.

A drawback of the MP2 method is that it overbinds molecules, meaning that bond lengths are too short and reaction barriers are commonly overestimated. It also overestimates π-π -interactions [49, 50] but describes hydrogen bonds well. [51] Grimme's proposal, a spin-component-scaled version of the MP2 method (SCS-MP2), [52, 53] overcomes part of the problems but on the other hand, underestimates the hydrogen bonds that are well described by the conventional MP2 method. In a large benchmark set for main group elements (GMTKN30), [54] the average error compared to more accurate methods (mainly CCSD(T)) for reaction energies was found to be 3.6 and 1.8 kcal/mol for the MP2 and the SCS-MP2 methods, being a significant improvement over the HF method (9.7 kcal/mol). Transition metal complexes having nearly de-

generate orbitals can be very problematic for the MP2 method because the HF wave function is not always qualitatively correct. [55]

2.4.1.3 Coupled Cluster Theory

Chemical accuracy means that that the errors in reaction energies and barriers should be less than 1 kcal/mol. In order to reach this, the most successful methods which account for dynamic electron correlation are based on Coupled Cluster (CC) theory. [56, 57] In the CI method, the wave function is presented as a linear combination of Slater determinants (Equation 2.8). The CC method uses an exponential ansatz to describe the wave function:

$$\Psi_{\mathrm{CC}} = e^{\hat{T}}\phi_0, \tag{2.10}$$

where $\hat{T}$ is a cluster operator, which is a sum of all possible excitation operators ($\hat{T} = \hat{T}_1 + \hat{T}_2 + ...$). The $e^{\hat{T}}$ can be presented as an Taylor expansion:

$$e^{\hat{T}} = 1 + \hat{T} + \frac{\hat{T}^2}{2!} + \frac{\hat{T}^3}{3!} + ... \tag{2.11}$$

This is extended by introducing the cluster operator with all possible excitations:

$$e^{\hat{T}} = 1 + \hat{T}_1 + \left(\frac{\hat{T}_1^2}{2!} + \hat{T}_2\right) + \left(\frac{\hat{T}_1^3}{3!} + \hat{T}_1\hat{T}_2 + \hat{T}_3\right) + ..., \tag{2.12}$$

where the excitation operator $\hat{T}_n$ includes all nth order excitations similarly to the CI method. It is important to notice from Equation 2.12 that the excitations are included as optimized, connected clusters ($\hat{T}_1$,$\hat{T}_2$,$\hat{T}_3$, etc.) but also as products (disconnected clusters) of lower excitations, i.e. triple excitations are also formed from the term $\hat{T}_1\hat{T}_2$. In practice, this means that the excitations can be truncated to a finite order but the higher excitations are still included. An important consequence is that, due to inclusion of the higher terms, CC theory is size consistent at any order. In commonly used form, the CC-methods are not variational but, identically to the CI-method, the exact solution can be approached by inclusion of higher order excitations.

The coupled cluster methods are named according to the optimized excitations they include. Inclusion of single and double excitations leads to the CCSD method. The CCSD method scales as N^6 and recovers approximately 90 - 95% of the correlation energy. [6] Whereas the MP2 method is known to overestimate π-π -interactions, the CCSD method underestimates them significantly. [51]

Inclusion of the triple excitations does not only increase the accuracy but

also the computational cost, providing a scaling of N^8. A popular way to increase the accuracy of the CCSD method is to include the triple excitations as a perturbation. The so formed CCSD(T) method has been proven to reach chemical accuracy in most cases and is considered to be the *Golden Standard in quantum chemistry*. [58] The CCSD(T) method is computationally already very demanding, and because of its poor scaling N^7, its applications are restricted to rather small systems.

Currently, a large amount of effort is being put in to the development of local correlated CC methods to obtain a major increase in speed without a loss of accuracy. [59–71] This has also enabled the use of CCSD and CCSD(T) level calculations in reaction mechanism studies. [72, 73] A recent highlight in the development of local correlated methods was reported by Riplinger and Neese. [74] The CCSD(T) method based on a 'domain-based local pair natural orbital approximation', DLPNO-CCSD(T), is nearly linear scaling with the respect of the system and was shown to recover practically the same amount of electron correlation as the conventional canonical CCSD(T) method. It has also been shown to produce very accurate thermodynamic results for large transition metal complexes. [75] Applications of these rapidly evolving methods for large systems have been reviewed recently. [76] However, these local correlated methods are mainly employed for single-point energy calculations on structures obtained using more approximate methods.

2.4.1.4 Frozen core approximation

One general approach to reduce the computational cost when accounting for dynamic correlation is the frozen core approximation, which means that the core electrons are left inactive during the correlation treatment. While the core electrons do contribute to the total correlation energy, this energy does not usually change much in chemical reactions where only the valence electrons are rearranged. Chemists are interested in relative rather than absolute energies, and therefore the error introduced by the frozen core usually cancels out when studying reactions. Since the common basis sets are designed to describe valence electrons accurately, specially designed core-correlated basis sets are needed if core-correlation is to be included. However, the core-correlation contributions can not always be neglected. [77, 78]

2.4.1.5 Size consistency

Size inconsistency was briefly described in 2.1. Its origin is easily understood when comparing the electron correlation between the CID and the CCD methods, where only the latter is size consistent. A system constructed from two

non-interacting subsystems of **A** should have the same energy as two such independent subsystem **A**. However, truncated CI methods such as CID treat electron correlation unequally in these two computations.

Both the CID and CCD methods only include double excitations. The CID and CCD wave functions for the two electron, two orbital system **A** are illustrated in Fig. 2.3. The wave function is constructed from the HF determinant and one excited determinant. To obtain the same electron correlation for the non-interacting system **A** + **A**, exactly the same excitations, as well as their combinations, should be taken into account.

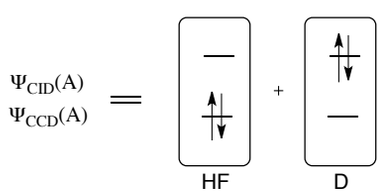

Fig. 2.3 The CID and CCD wave functions for the system **A**.

The corresponding determinants for system **A** + **A** are shown in Fig. 2.4. The electron configuration in which both subsystems would be doubly excited at the same time is formed from a quadruple (Q) excitation, and this is absent in the CID wave function. Therefore, the non-interacting system **A** + **A** does not have the same energy as 2**A**. The CCD method contains higher excitations as products of the lower ones and the Q excitations are included. This is not just a problem in non-interacting systems; it becomes crucial in a single molecule with increasing system size.

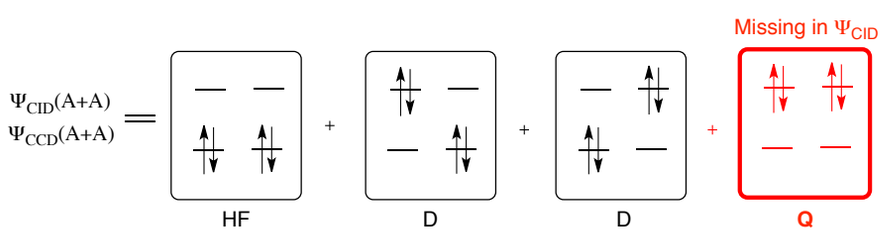

Fig. 2.4 The CID and CCD wave functions for the system **A** + **A**.

2.4.2 Static Correlation

The electron correlation energy was previously defined as a small correction to the energy caused by the tendency of an electron to respond to the rapid movement of other electrons. This is taken into account when treating dynamic electron correlation. Static correlation is a long range correlation effect

required to describe systems where a single Slater determinant does not give a qualitatively correct description of the electron configuration. [8] These are common cases where other low-energy electron configurations exist which are nearly degenerate with the HF solution. In general, static correlation is not important for closed-shell molecules at their equilibrium geometries, but may be crucial at distorted geometries. Transition metal (TM) complexes may also be very challenging for HF-based theories due to the need for static correlation.

2.4.2.1 Complete Active Space SCF

The most common computational approach for taking static correlation into account is the Complete Active Space SCF method (CASSCF). [79, 80] In the CASSCF method one chooses an (n, m) active space, constructed from n electrons in m orbitals, and performs a full CI computation in this space. Unlike in the CI method, not only the excitation coefficients (Equation 2.8) are optimized but the orbitals are also fully relaxed. The CASSCF method is both variational and size consistent.

A problem with the CASSCF method is that electron correlation is only treated in the active orbitals and as a consequence, the CASSCF method overestimates the stability of biradicals. To obtain a balanced treatment of the whole system, a full valence active space could be employed but, due to the factorial raise in the computational cost, this is not always a plausible option. A common approach is to add dynamic correlation by perturbation on top of the CASSCF solution. Examples of such methods are the Complete Active Space Second Order Perturbation Theory (CASPT2) [81] and the N-Electron Valence State Perturbation Theory (NEVPT2) [82] methods. The CASPT2 method has been found to be successful in describing reactions where concerted and stepwise reaction mechanisms compete. [83–85] As a specific example, the Cope rearrangement can be considered as having a concerted transition state, or to go through a reaction pathway involving biradical intermediates. [86]

The inactive part of the CASSCF method is the HF solution and it scales as N^4. With a small active space this is the limiting factor but, with an increasing active space size, the number of configurations increases factorially as illustrated in Table 2.2. With modern algorithms a (12,12) active space (12 electrons in 12 orbitals) single point energy calculation is still comfortably achieved, but in larger active spaces, the number of possible configurations is too large.

The amount of active orbitals allowed in the CASSCF method may not always be sufficient even for medium size molecules, especially when studying excited states. [87, 88] In the restricted active space SCF (RASSCF) method, the system is divided in three subspaces, RAS1-RAS3, allowing inclusion of

Table 2.2 Size of the active space (n, m) and number of configurations for a singlet state.

(n, m)	Configurations
(2,2)	3
(4,4)	20
(6,6)	175
(10,10)	19404
(12,12)	226512
(14,14)	2760615

larger active spaces. [89, 90] The RAS2 subspace corresponds to the CASSCF active space where a full-CI computation is performed. The RAS1 and the RAS3 subspaces include occupied and unoccupied orbitals, respectively, where a truncated CI computation is performed. Dynamic correlation can be included further in the RASPT2 method. [91] A new promising method is the Density Matrix Renormalization Group (DMRG) algorithm which allows inclusion of very large active space to obtain similar results to the CASSCF method. [92,93]

The choice of active space is non-trivial and requires expertise from the user. To assist with the selection, Björn Roos, the father of CASPT2, has published his own useful instructions. [94]

2.4.3 Need for static correlation?

Recovering the dynamic part of the electron correlation relies on having qualitatively correct HF orbitals. Without this, the calculations become meaningless. Even the golden standard CCSD(T) can yield extremely poor results if the HF reference configuration is not sufficient. [76]

A good warning sign are the populations obtained from relaxed natural orbitals. Any orbitals having an occupation number between 1.95 and 0.05 should be considered carefully for static correlation. The orbitals obtained from a computation that takes into account the dynamic part of the electron correlation with the described methods are normally the HF orbitals and the natural orbitals need to be computed separately.

Lee and Taylor [95] suggested T_1 diagnostics from a CC calculation as an indicator of the static correlation. In practice, this gives information on how much single excitations contribute to the electron correlation. If this value is larger than 0.02, the effect of static correlation should be investigated. This can be understood when considering that the single excitations contribute most to relax the HF orbitals. If the contribution of single excitations to the electron correlation is large, the HF orbitals are not sufficient for an electron

correlation treatment. For example, Thiel and coworkers showed the UHF orbitals to be problematic for some iron-complexes, leading to a notable error in the CCSD(T) potential energy surface (PES). [96]

Another tool for diagnostics exist: The D_1 and D_2 amplitudes from CCSD and MP2 calculations are claimed to be more reliable than the T_1 diagnostics because they are independent from the system size. [97,98] The D_1 amplitudes are a measure of orbital relaxation similarly to T_1 diagnostics but employ slightly different formulation. The D_2 amplitudes, on the other hand, alert the user if low-lying doubly excited states exist. Based on D_1 and D_2 amplitudes, the quality of MP2 and CCSD treatment can be considered excellent with the following cut-offs: $D_1(\text{MP2}) \leq 0.015$; $D_1(\text{CCSD}) \leq 0.020$; $D_2 < 0.15$.

To give a further illustration of these problems, the importance of static correlation is highlighted in two simple reactions: homolytic dissociation of H_2 and *cis-trans* isomerization of ethene.

2.4.3.1 Dissociation of H_2

Homolytic dissociation of H_2 is a good example for understanding the importance of static electron correlation when bonds are broken or formed. Let us first consider how the orbital structure of H_2 in a minimal basis set changes during the dissociation (Fig. 2.5).

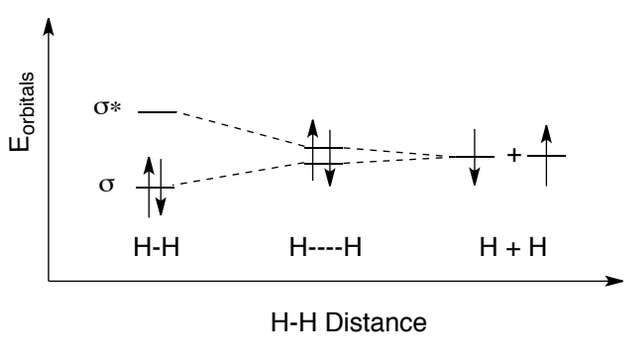

Fig. 2.5 Orbital view for the dissociation of H_2.

At the equilibrium bond length, both electrons occupy the same molecular orbital (MO) to form a σ-bond. The lowest unoccupied molecular orbital is the corresponding antibonding σ^*-orbital. In the course of the dissociation, the energy gap between the orbitals decreases, electrons move in to separate orbitals and the bond is broken. In order to describe the potential energy surface (PES) correctly for homolytic dissociation, the method should be able describe the electron configurations where:

- the σ-orbital is doubly occupied

- the σ and σ^* orbitals are nearly degenerate and electrons occupy the both orbitals
- the hydrogens are present as two non-interacting radicals in an electronic singlet state.

The potential energy surface for the reaction computed using various WFT methods is shown in Fig. 2.6. The basis set used in the computations is a triple-ζ quality def2-TZVPP (See section 2.7 for details). For this specific example, the CCSD method gives the exact solution, taking into account all possible excitations of both electrons.

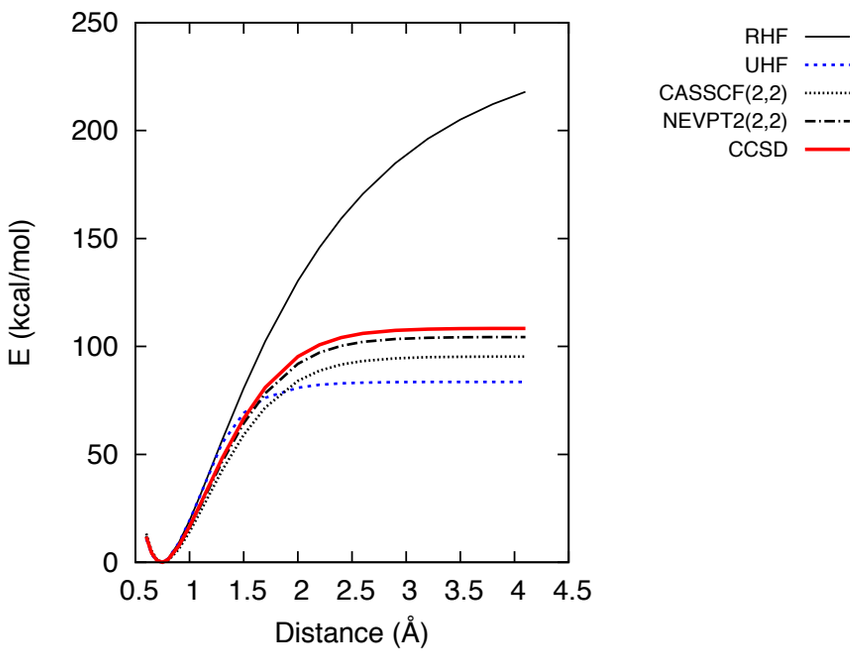

Fig. 2.6 Dissociation of H_2 using various methods.

The RHF calculation leads to a description of the dissociation, which is 50% homolytic and 50% heterolytic and therefore overestimates the gas-phase reaction energy significantly (Fig. 2.6 and section 2.3.2). The UHF method produces a PES which dissociates correctly but the wave function is no longer a true spin state: The $\hat{S}^2$ value of 1 implies that the wave function to be an even superposition of the singlet and the triplet states. The underestimation of the bond dissociation energy (BDE) is typical for the UHF method, as it does not treat the non-interacting diradical and covalently bound molecule equivalently. [5] In this case, the UHF method gives the correct description of the dissociated product because there is no electron correlation in two non-interacting single-electron systems. However, by neglecting electron correlation

in the molecule, the UHF method underestimates the dissociation energy of H_2. Thus neither method results in a properly-described PES at all values of bond length.

A straightforward approach is to include static correlation in the RHF solution using the CASSCF method. Chemically the most important orbitals are the σ and σ^* -orbitals. If the electron excitations are restricted to two electrons in these orbitals, the method is called CASSCF(2,2) and treating the static correlation in these orbitals reduces the RHF energy significantly. In a minimal basis set, the H_2 molecule has only two orbitals and therefore the CASSCF(2,2) method would provide the exact solution. In this case, a larger basis set has been used to elucidate the effect of dynamic correlation on higher unoccupied orbitals, which is seen as the energy difference between the CASSCF and CCSD results.

Dynamic correlation is added to the CASSCF solution with a second-order perturbative treatment by employing the NEVPT2(2,2) method. The dynamic correlation increases the reaction energy, confirming that the CASSCF method overstabilizes diradical species. It should be noted that, while the CCSD presents the exact solution for this specific problem, it should not be used as a standard. The success of the CCSD method here is due to choosing a two-electron system and the NEVPT2 method is more applicable for a wider variety of systems.

2.4.3.2 *Cis-trans* isomerization of ethene

The *cis-trans* isomerization of ethene provides another illustrative example of the correlation effects. The important π and π^* orbitals are presented in Fig. 2.7. As in the previous example, two orbitals become degenerate in the course of the isomerization and in order to describe the reaction correctly, this needs to be taken into account.

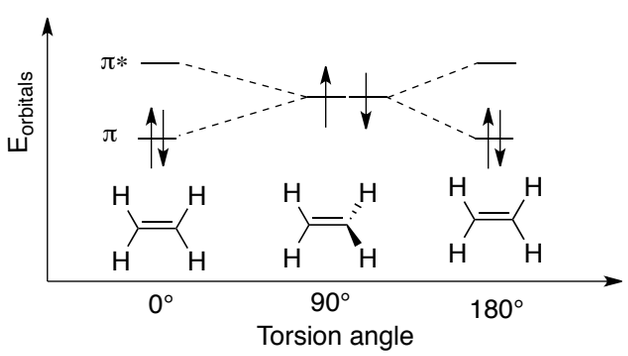

Fig. 2.7 Orbital view of *cis-trans* isomerization of ethene.

The calculated PES using various methods is shown in Fig. 2.8. For this example, the exact solution taking into account all electronic excitations is no longer presented due to the increased system size (16 electrons). In the previous example, we noted that the NEVPT2 method is capable of treating both static and dynamic correlation to approach the exact solution, and therefore acts as a reference in this case.

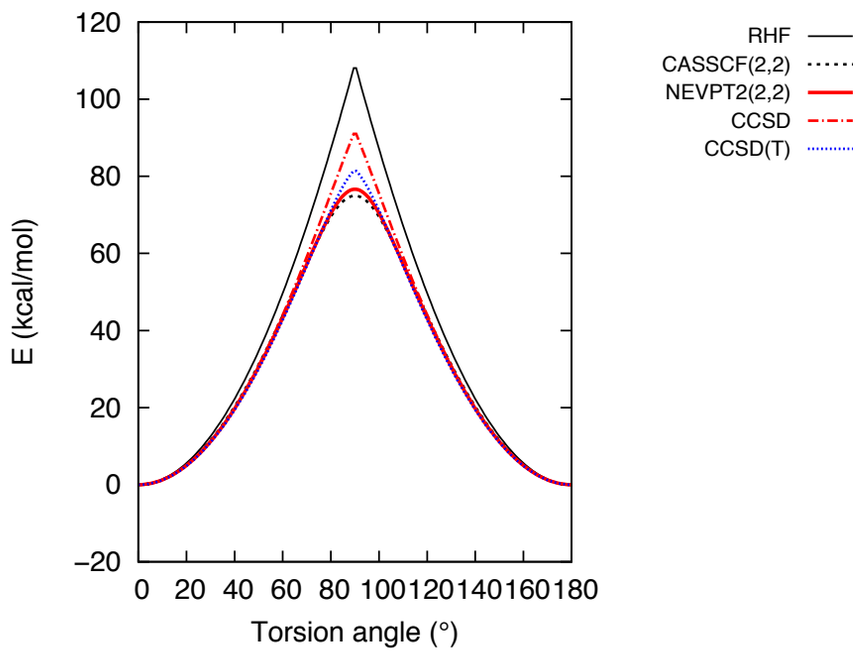

Fig. 2.8 *Cis-trans* isomerization of ethene with different methods.

The RHF method overestimates the barrier significantly, but it is also unable to describe the PES smoothly close to the transition state. Inclusion of single and double excitations improves the result slightly but the CCSD method suffers from the same problems. The result is further improved with inclusion of perturbative triples (CCSD(T)) but is still not very accurate. The CASSCF(2,2) method overstabilizes the biradical transition state slightly.

It is clear that the solution is exact if all possible electronic excitations are taken into account. When the system size increases, this is no longer anymore possible due to practical reasons. Therefore understanding the problem and treating the static correlation correctly is of significant importance. The 'failure' of the golden standard is already seen in this simple example where the HF reference wave function breaks down.

2.5 Density functional theory

So far this chapter has focused on wave function-based *ab initio* methods. Another very popular approach is to compute the energy and properties of the system using density functional theory (DFT). [99–101] In 1964 Hohenberg and Kohn proved that the ground-state electron density determines the electronic energy of the system according to the variational principle. [102] This is an enticing result, as the electron density is dependent on 3 spatial coordinates instead of the $3n$ spatial coordinates of the wave function, where n is number of the electrons in the system. However, the exact functionals which connect the kinetic energy and the electron-interaction energies to the electron density are not known.

In 1965, Kohn and Sham formed the basis for modern KS-DFT, where a set of self-consistent equations are solved to find a set of spin orbitals. [103] The exact KS-DFT equation is given by:

$$E_{\mathrm{DFT}}[\rho(\mathbf{r})] = T_e[\rho(\mathbf{r})] + J_{ee}[\rho(\mathbf{r})] + V_{Ne}[\rho(\mathbf{r})] + E_{xc}[\rho(\mathbf{r})]. \tag{2.13}$$

This is the functional that connects the electron density to the electronic energy of the system. The nuclear-electron attraction term V_{Ne} can be solved exactly and $J_{ee}[\rho(\mathbf{r})]$ is the classical Coulomb electron-electron repulsion of the electron density with itself. The kinetic energy of all electrons is described in the first term $T_e[\rho(\mathbf{r})]$. To solve it, it is described as the kinetic energy of a hypothetical system of non-interacting electrons, having the same density as the true system of interacting electrons.

The last term, the exchange-correlation functional, is a functional that corrects all the approximations made to the kinetic energy and the electron correlation to yield the exact solution, i.e., with the true exchange-correlation functional, the obtained solution would be exact. A disadvantage of the KS-DFT is that the exact exchange-correlation functional is not known. A main advantage, on the other hand, is that DFT approximately includes electron correlation. The physical meaning of the KS-orbitals can be argued [104, 105] but, they can be said to be qualitatively improved over HF orbitals and in some cases they even provide a more sufficient basis for WFT-based electron correlation treatments. [96]

The procedure for solving the KS equations is very similar to the scheme used to solve the Hartree-Fock equations: Solve the orbitals that minimize the energy. In the HF method, the electrons interact with the effective field describing the average positions of the electrons, whereas in DFT, the potential is constructed from the electron density of noninteracting electrons, having the

same density as the real system of interacting electrons.

2.5.1 DFT functionals

Because the exact functional has not been derived, approximate functionals (or methods) approach the problem in various ways. The commonly employed functionals are based on one of several common DF approximations (DFA) which may be described as LDA, GGA and meta-GGA, as well as hybrid and double hybrid functionals (DHF). [100] Modern algorithms have enabled the use of different variants of RI-appoximation with all approximations providing a significant speed-up. Non-hybrid RI-DFT scales as N^3, and is therefore potentially even faster than the HF method. The computational cost of hybrid-DFT is similar to the HF method and double-hybrid methods have similar computational costs as the MP2 method.

2.5.1.1 LDA functionals

In the local density approximation (LDA), the exchange-correlation energy is defined as:

$$E_{xc}^{\mathrm{LDA}}[\rho] = \int \rho(r)\varepsilon_{xc}(\rho)d\mathbf{r} \tag{2.14}$$

The electron density ρ of the system can be presented as a function depending on each spatial coordinate r. The exchange-correlation functional connects this function to the function that describes the exchange-correlation energy ε_{xc} of an electron in a uniform electron gas with a density ρ. In the local spin density approximation (LSDA), the spin is also included in Equation 2.14 to allow separation of the α and β spin densities. The LDA is actually surprisingly useful in modeling periodic metal systems where the electron density of the system varies gradually. [106] In molecular applications it gives reasonable structures, but it tends to overbind molecules significantly and is therefore not a practical choice for chemical problems. [101, 107]

2.5.1.2 GGA and meta-GGA functionals

The next step to improve the description of the LDA is to include the gradient (the first derivative) of the electron density in the exchange-correlation functional. The result is called the generalised gradient approximation (GGA) and for molecules it represents a significant improvement over the LDA. Examples of such functionals are e.g. PBE [108] and BP86 [109,110]. To improve the functional further, the kinetic energy density and other higher derivatives can be added to GGA functionals. These functionals belong to the class of

meta-GGA functionals, and the TPSS-functional [111], commonly employed in this work, belongs to this family. The accuracy of the meta-GGAs has been shown to be only a small improvement over GGAs, but on the other hand, the computational cost is also very similar. [54]

2.5.1.3 Hybrid and DH functionals

One can confidently state that most DFT functionals used in computational organic chemistry belong to the family of hybrid functionals. These functionals are formed by combining the GGA or meta-GGA functional with a fraction of the exact electron exchange energy from the HF theory. Examples of commonly used functionals in this category are B3LYP [112,113], PBE0 [114] and PW6B95 [115].

Traditionally, DFT is a theory of occupied orbitals because these determine the electron density. The virtual (unoccupied) orbitals are taken into account in DHFs by including a fraction of the MP2-correlation energy into the hybrid functional. An example of a double hybrid functional used in this work is B2PLYP. [116] There are also other approaches to include the virtual space, e.g. the random phase approximation. [117]

2.5.2 DFT-D3

The exchange-correlation functional includes electron correlation but, unlike the wave function-based *ab initio* methods, there is no systematic way to approach the 'Full CI' solution. Practically, all common DFAs treat only short-range correlation effects and give poor descriptions of dispersion interactions. [118,119] For instance, the B3LYP PES for benzene dimers is completely repulsive, rather than having a physically correct π-π stacked minimum. Several approaches exist to correct this problem. [119,120]

In this work, all DFT functionals have been used in combination with the atom pair-wise correction method of Grimme, denoted as DFT-D3 [121]:

$$E_{\text{DFT-D3}} = E_{\text{KS-DFT}} + E_{\text{disp}}. \tag{2.15}$$

Here, the dispersion interactions are simply treated as an external correction to energy and gradient, but not to the properties. The E_{disp} is:

$$E_{\text{disp}} = -\sum_{AB}\sum_{n=6,8} s_n \frac{C_n^{AB}}{r_{AB}^n} f_{\text{damp}}(r_{AB}), \tag{2.16}$$

where the coefficient C_n^{AB} is defined for each atom pair and s_n for different functionals. The $n = 6$ and $n = 8$ terms aim to describe the long-range and mid-range correlation, with r^{-6} and r^{-8} behaviors, respectively. To avoid

double counting of close-range correlation effects, E_{disp} is damped at a certain cut-off distance with a damping factor f_{damp}. Two schemes exist: The original D3 employed zero-damping where the E_{disp} is damped to zero, and in the newer D3(BJ) approach, [38] the E_{disp} term is damped to a constant value proposed by Becke and Johnson. [122–124] The choice of the damping function can be specific for the system and the functional, but as a general recommendation, the HF method should only be used with D3(BJ). [38] The D3-method also includes three-body -dispersion correction for single point energies, which might be important for describing large supramolecular complexes properly. [49]

It should be noted that the observed poor description of medium-range correlation and neglecting the long-range correlation does not only affect weakly interacting complexes, and pure DFT suffers from the same problems as the HF method when it comes to e.g. alkane isomerization and bond dissociation energies. [5, 32, 34, 118] The results are improved by using the D3-correction, but accounting for non-local correlation effects with DHFs in addition to D3 improves the result even more, albeit at high computational cost.

2.5.3 Self-interaction error

The HF method is based on the self-consistent field (SCF) where the electrons interact with an effective field that describes the average position of all electrons in the system. When computing the classical Coulomb electron-electron repulsion energy, the electron therefore actually interacts also with itself. This is called self-interaction error (SIE). When solving the Hartree-Fock-Roothaan equations, the SIE is exactly canceled out by the electron exchange energy.

In DFT, the electrons interact with a potential which is constructed from the whole electron density. In a similar fashion to the HF method, the electrons therefore interact with themselves. This effect would be canceled by the exact exchange-correlation functional, but as discussed earlier, this term is not known. Therefore DFT functionals suffer from SIE.

What does SIE mean in our computational applications? It can be understood in the classical example of dissociation of H_2^+, shown in Fig. 2.9, computed with the UHF method, PBE (GGA functional) and PBE0 (corresponding hybrid functional of PBE). The system is constructed from two protons sharing one electron. When the distance between the protons is increased, the system should dissociate to a proton and a hydrogen atom. The probability of both protons to accommodate the electron is equal as they are identical, i.e., both protons accommodate a fractional number of half electron.

For a one-electron system, the UHF method provides an exact solution (there are no electrons to correlate). The PBE functional underestimates the dissociation energy significantly because the electron interacts with itself by

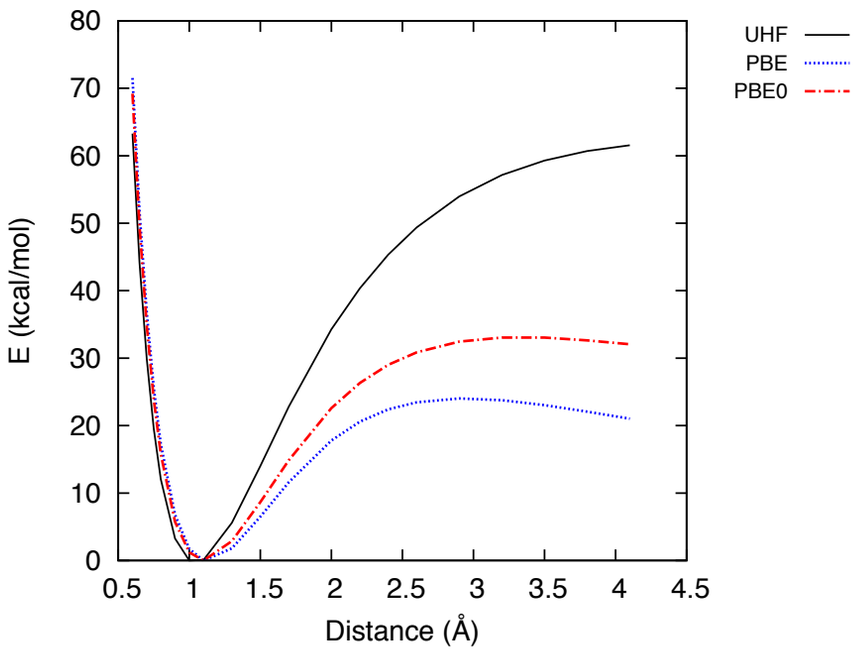

Fig. 2.9 Dissociation of H_2^+ molecule with different methods.

lowering the total energy. The hybrid functional PBE0 is slightly better. While this example may not seem important when considering 'real' systems, fractional occupation numbers in orbitals are relevant for transition states. Therefore, DFT functionals commonly underestimate reaction barriers. Hybrid functionals perform slightly better as the inclusion of the exact exchange cancels the SIE partly. The issue has also been discussed elsewhere as delocalization error. [125, 126]

Another drawback is artificial charge transfer. Due to the SIE, pure DFT functionals underestimate the energy difference between the highest occupied (HOMO) and the lowest unoccupied molecular orbitals (LUMO), also called the HOMO-LUMO -gap. This may artificially overstabilize structures existing as cation and anion. An anion often has a high-energy HOMO and a cation a low-energy LUMO. When this gap is small, artificial charge transfer may be observed, e.g. in ionic liquids. [127] Similar misbehavior has been observed for radical reactions where the energy gap between the singly-occupied molecular orbital (SOMO) and the LUMO is small. [128] The HOMO-LUMO and SOMO-LUMO gaps are increased by inclusion of the exact exchange and therefore hybrid functionals perform better if artificial charge transfer is observed, e.g. the hybrid functional PW6B95-D3(BJ) has been shown to provide accurate kinetic data for reactions involving aniline radicals. [129]

2.5.4 Accuracy of DFT

A typical approach to evaluate the accuracy of different functionals is to benchmark them against accurate *ab initio* results, such as CCSD(T), or experimental data. Perhaps the most comprehensive test set for main group thermochemistry, kinetics and non-covalent interactions is the GMTKN30, constructed from 30 individual test sets. [54] These cover basic properties, such as atomization energies and electron affinities, but also barrier heights and reaction energies of interest for organic chemists, e.g. for Diels-Alder reactions.

John Perdew has introduced a hierarchy of DFA accuracy in his famous 'Jacob's ladder of DFAs'. [130] The same hierarchy was observed within the GMTKN30 test set, in ascending order: LDA, GGA, meta-GGA, hybrid funtionals, and finally reaching the current limit with DHFs. All functionals except LDA were used in combination with D3. The DHFs were found to be even more accurate than the MP2 method and comparable in accuracy with the SCS-MP2 method. The DHFs show the lowest error in reaction energies (1.4 - 2.4 kcal/mol) followed by hybrids (2-3 kcal/mol for the best) and (meta-)GGAs performed slightly worse. The computational costs of the DHFs and the SCS-MP2 method are very similar, but the DHFs may benefit from faster basis set convergence. [54]

The GMTKN30 test set is constructed mainly from closed-shell small main group molecules, and the results may not hold for transition metal (TM) compounds. In several studies, the GGA and meta-GGA functionals have been noted to perform best for TM-complexes, whereas DHFs might provide rather poor results. [131–133] Inclusion of the exact exchange commonly increases the accuracy, but using a too large fraction might lead to spin-contamination. [96] The spin-state energetics of transition metal complexes may also be problematic for DFT. [134]

Overall, modern DFT-D3 is very successful in describing organic and organometallic systems, as well as weak interactions. [135–138] Conventional DFT underestimates hydrogen bond strengths, but inclusion of D3 improves the result, and almost MP2 quality is reached even for very weak hydrogen bonds. [139] Some functionals are heavily parameterized on a specific set of molecules or reactions, e.g. the popular M06 functional has been fitted to 36 parameters, [140, 141] and their accuracy may be very different from one system to another. DFT has its own fundamental issues as discussed in the text (see also ref. [142]), and the user should be aware of them. Similarly to the WFT methods, also static correlation needs to be treated properly if other low energy solutions exist.

2.6 Relativistic effects

Relativistic effects are not considered to be important in light main group chemistry due to the slow speed of the core electrons. In heavy-elements, the electrons in the $1s$-orbital approach the speed of light, and relativistic effects become important. [20] The $1s$-orbital is contracted and the effect is transferred to all s- and p-orbitals. For instance, the most strongly- contracted orbital for gold is $6s$ instead of $1s$. [19] Because s- and p-orbitals contract towards the nuclei, they are stabilized. In contrast, the d- and f-orbitals are expanded and destabilized. The shifts in the orbital energy levels are specified as scalar relativistic effects (SR) (Fig. 2.10). The fully-relativistic effect (FR) also includes spin-orbit coupling (SOC), where all orbitals with angular momentum of $l > 0$ (p, d, f) are divided into two different energy levels. In this work, computations have been performed for cobalt and gold complexes, where relativistic effects are well known to be important for the latter.

The chemistry and properties of gold are strongly influenced by relativistic effects. [143–145] For example, the commonly used $AuCl_3$ would not even be stable in the 'non-relativistic' world, [146] and the strong Lewis-acidity of gold is due to scalar relativistic effects. [147] Pernpointner noted that the relativistic treatment of gold complexes can be restricted to the scalar relativistic level, while the SOC does not influence the orbital populations or energy levels. [148]

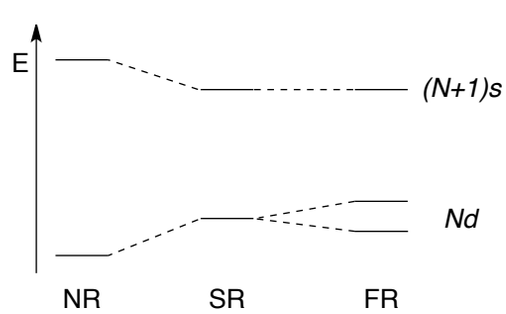

Fig. 2.10 The relativistic effect for the Nd-shell and $(N+1)s$-shell. NR = Non-relativistic, SR = Scalar-relativistic, FR = Fully-relativistic.

In the current work, the scalar relativistic effects have been taken into account using two variants: a relativistic effective core potential (RECP) [149] for gold; and the zeroth-order regular relativistic approximation (ZORA) [150] for all atoms. The RECP treats the core electrons as a fitted pseudopotential, and only the valence electrons are treated explicitly. Whereas the RECP can be considered as a relativistic 'add-on' to a non-relativistic computation, in the ZORA approach, relativity is taken into account for all atoms in the

Hamiltonian. Although in some cases the ECPs have been noted to recover only part of the relativistic effects, [151] the results obtained during the initial tests of this work were very similar when comparing both approaches.

2.7 Basis set

Quantum chemical methods are based on optimizing the electronic structure of the molecule in various ways. In all the approaches described here, the electrons are placed in molecular orbitals, which are constructed from atomic orbitals through linear combination. The atomic orbitals are described by *basis sets*, constructed from *basis functions*. Two popular types of basis functions exist: Slater-type orbitals (STOs) and Gaussian-type orbitals (GTOs). [5–7]

Slater-type orbitals are basis functions that mimic the exact solution of the Schrödinger equation for the hydrogen atom. Currently, these are rarely used as most of the current quantum chemical programs rely on Gaussian-type orbitals. The difficulty with STOs in molecular calculations is that solving some of the necessary integrals analytically is practically impossible, requiring them to be evaluated numerically.

These computational difficulties are avoided with Gaussian-type orbitals. As a disadvantage, a single GTO does not describe the solution for a one-electron atom correctly. Therefore multiple GTOs are needed to describe one basis function, whereas each STO correspond to a basis function. The common basis sets have recently been reviewed comprehensively [152, 153] and only a short overview is given here.

2.7.1 Basis functions

To construct a basis set, the electron configuration of an atom is considered, i.e. $1s^2 2s^2 2p^2$ for carbon. The minimal requirement for the basis set is that each occupied atomic orbital should be described with a single basis function, meaning that the respective basis set for carbon should have two s-type functions ($1s^2$ and $2s^2$) as well as p_x, p_y and p_z -type functions. Each of these basis functions may consist of several GTO's. A basis set fulfilling these minimum requirements, is called a minimal basis set or single-ζ (SZ).

The use of only one basis function to describe an orbital of an atom in a molecule is not very accurate, especially for delocalized valence electrons. To produce a more accurate basis set, a straightforward approach is to increase the amount of basis functions used to describe an atomic orbital. A double-ζ (DZ) basis set has 10 (4 s-type and 6 p-type) basis functions for carbon instead of 5. The accuracy can be further increased in triple-ζ (TZ), quadruple-ζ (QZ) etc. basis sets.

The number of basis functions, and the computational effort, rises quickly with increasing size of the basis set. To find a compromise between accuracy and cost, Pople has developed split-valence basis sets, [154] where the core and valence electrons are treated separately. The core-electrons are described with a minimal basis set whereas a larger amount of basis functions are used to describe chemically important valence electrons. A split-valence basis set of DZ quality for carbon treats the 1s -orbital as SZ-quality whereas valence-electrons ($2s$ and $2p$ orbitals) are treated as DZ. Thus, the split-valence basis set for carbon is built from 9 basis functions instead of 10.

To provide more flexibility for the electrons to delocalize, polarization and diffuse functions can be added. For instance, including only s-type functions for hydrogen means that the electron distribution around the nucleus is always spherical whereas in real molecules hydrogens are polarized. To take the polarization effect into account, functions having angular moment one greater than the valence space are added. For hydrogen this means additional p-type functions and for carbon d-type functions. Diffuse functions, having the same angular momentum as the valence space, are added to allow outer electron shells to expand, which is especially important in anions.

The convergence of the energy with respect to basis set size is of key importance, as the accuracy of the result is dependent on it. In general, the HF and DFT methods can be considered to give properties and relative energies corresponding to the complete basis set (CBS) limit with a TZ quality basis set and qualitatively correct results may already be obtained at the DZ level. The basis set requirement is higher for methods that include electron excitations, i.e. WFT methods that include dynamic correlation and the DHFs. In these cases, at least a TZ level basis set should be used but one should be aware that even a QZ level basis set might not be sufficient. Therefore a good practice is always to check the convergence of the result compared to higher quality basis sets.

2.7.2 Basis set families

Different basis set families differ from each other with regard to how the basis functions are optimized. In this work, the so-called Karlsruhe split-valence basis sets, denoted with prefix def2-, have been employed. [155,156] This basis set family has two major benefits: It is available for the whole periodic table up to radon (Z = 86) and includes consistent auxiliary basis sets to benefit from the RI-approximation. [157] Basis sets are named as def2-SVP, def2-TZVP and def2-QZVP for valence DZ, TZ and QZ, with P indicating added polarization functions. RECPs are included in the basis set from row five onwards. With ZORA, modified, all-electron scalar relativistic version of the

def2-basis sets have been used, and these are referred to later using the -ZORA suffix. [158–161]

The original implementation of the def2-basis set did not include diffuse functions. These have been added later, independently by the groups of Furche [162] and Truhlar [163]. The authors recommend including them when studying response properties [162] and electron affinities [163] but non-covalent interactions and barrier heights are not affected significantly. A common recommendation is to always include diffuse functions when studying anions, but Truhlar and coworkers note that the def2-basis sets are more diffuse than other commonly used basis set families.

A very popular split-valence basis set is the 6-31G basis of Pople and coworkers. [164] The dash separates the core and valence electrons to the left and right sides, respectively. Each individual number is a basis function being constructed from gaussian functions defined by the value of the number: the core-electrons are described with single basis function (SZ) constructed from 6 gaussian functions and the valence-electrons are described by two basis functions (DZ) where the inner function is composed of three gaussians and the outer function is a single gaussian function. A TZ basis set of this family is named 6-311G. Polarization functions are denoted as * and diffuse functions as +. A disadvantage of this basis set family is that it is not available for the whole periodic table, e.g. for transition metals.

Another commonly used basis set family is the Dunning's [165] split-valence aug-cc-pCVNZ basis set. These split-valence basis sets (N = D,T,Q etc.) are optimized to recover the maximum amount of electron correlation. The diffuse and core-correlation functions, denoted with the prefix *aug* and C, are optional but polarization functions are optimized in the basis set. These basis sets are used mainly with electron correlated WFT methods, while for DFT, the previously mentioned families are much more efficient.

2.8 Solvent effects

In the past, practically all quantum mechanical computations were performed in vacuum. Even though these conditions are far from the solvent-phase experiments, the so-called gas phase approximation has proved to be very succesful. It does not mean that solvation does not affect the real system, but rather that the effect on different reaction pathways is similar and therefore the error cancels out when comparing e.g. regio- and stereoselectivities. This does not always hold, e.g. if ionic and neutral structures compete. Therefore, depending on the system and focus of the study, solvation effects may need to be considered.

To describe solvent effects properly, the optimal approach would be to capture the dynamic and macroscopic effects of the solvent using an accurate computational level. To achieve this, one should not only involve thousands of solvent molecules in the calculations, but also sample the average behavior and movement of these. A common approach is to take the solvation effects into account by an implicit solvent model, which simulates a dielectric cavity, parameterized with the macroscopic properties of the solvent. [166–169] Another often-employed strategy is to describe the macroscopic properties of the solvent with an implicit model and to add a few explicit solvent molecules to describe specific solute-solvent interactions, e.g. hydrogen bonding. For reaction energies and barriers, this method might however, lead to errors if the conformational freedom of the system is not included correctly. One should also consider that the properties of an isolated solvent molecule may be very different from the bulk solvent.

In this work, the solvent has been described with the conductor-like screening model (COSMO). [170] A major limitation of COSMO, and most implicit solvent models, is that they only take into account the average electrostatics of the solvent according to its macroscopic dielectric constant. Therefore, specific π-π or hydrogen bonding interactions between the solvent and the solute are not described properly. In cases where hydrogen-bonding is apparent, COSMO for real solvents (COSMO-RS) has been applied. [171, 172] The theoretical background of both methods has been reviewed recently. [173] COSMO-RS has been shown to be a great improvement over COSMO, [174, 175] although it is still not quantitatively accurate for describing hydrogen bonding. [176]

2.9 Transition State Theory

The energies can be linked to experimental reaction or catalyst design via transition state theory (TST), [177] where the minimum energy structures are connected to each other via transition states (TS): The TS are saddle-points in the PES and maximum energy points on the reaction pathway. For example, the reaction profile for reaction **A** + **B** → **A-B** is shown in Fig. 2.11.

The energies are specified as Gibbs free energies, constructed from enthalpy and entropy ($G = H$ - TS). The energy difference between the starting state (**A** + **B**) and the transition state (**A**–**B**)‡ is defined by the Gibbs free activation energy $\Delta G^{\ddagger}$. The overall reaction energy is defined as the energy difference of (**A**+**B**) and **A**–**B** and termed as ΔG.

The obtained $\Delta G^{\ddagger}$ values can be linked to reaction rates using the Eyring

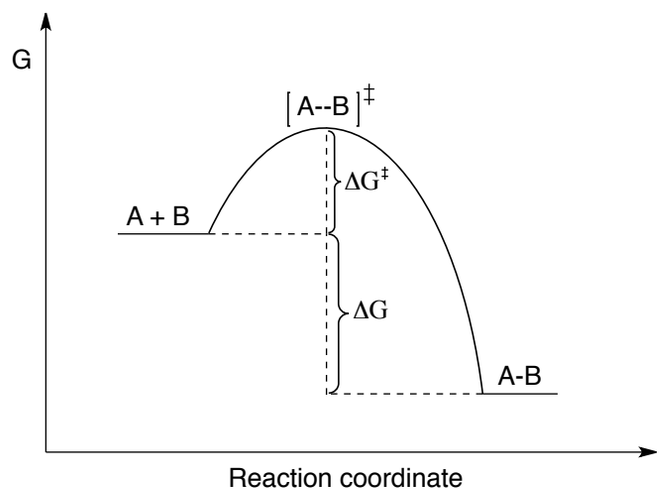

Fig. 2.11 The reaction profile for a reaction between **A** and **B**.

equation [178]:

$$k = \frac{k_B T}{h} e^{-\frac{\Delta G^{\ddagger}}{RT}}, \tag{2.17}$$

where k_B is the Boltzmann constant; h is Planck's constant; R is the molar gas constant; and T is the temperature in Kelvin. According to the Boltzmann distribution, different energy states are populated according to $e^{-\Delta G/(k_B T)}$. For example, if five conformers exist with nearly degenerate energies, their relative populations can be evaluated from:

$$\frac{\mathrm{Pop_1}}{\mathrm{Pop_n}} = \frac{e^{-\frac{\Delta G_1}{k_B T}}}{\sum_n e^{-\frac{\Delta G_n}{k_B T}}}. \tag{2.18}$$

In equation 2.18, one calculates the population of conformer 1 ($\mathrm{Pop_1}$) compared to all five conformers (n = 1,2,3,4,5). This is a useful formula for calculating e.g. regio- and enantiomeric ratios, defined by the $\Delta\Delta G^{\ddagger}$ between different transition states in the case of kinetic control.

With these tools, the computed energies can be linked to experimental reaction rates or relative populations. To illustrate the accuracy needed in the computations, rate constants for three different $\Delta G^{\ddagger}$ values from the Eyring equation are shown in Table 2.3.

The behavior of the rate constant compared to the energy barrier is exponential. Therefore even small errors in the computed $\Delta G^{\ddagger}$ values will introduce significant errors in the computed rate constants. Also the energy obtained from computations after common approximations is not the Gibbs free energy of the system. The quantum chemically computed energy is based only on

Table 2.3 Reaction rates calculated from Eyring equation at 298.15 K.

$\Delta G^{\ddagger}$ (kcal/mol)	Rate (s^{-1})
10	287000
15	61
20	0.01

the electronic energy and the nuclear repulsion energy at 0 K, and does not take into account the vibrational and rotational movement of the nuclei. To obtain the Gibbs free energies for a specific structure, vibrational frequencies of the system are computed from second derivatives of the energy with the respect to nuclear coordinates and solving the nuclear BO equation. The thermal corrections are then obtained from statistical mechanics by applying the *Rigid-rotor Harmonic-Oscillator* approximation to the quantized vibrational frequencies and energy levels. The vibrational frequencies and thermal corrections calculated in this way are typically slightly overestimated due to the harmonic approximation, since the experimental, real vibrational frequencies are anharmonic. [6] The overestimation of the harmonic vibrational frequencies is usually systematic and they may be scaled using an empirically defined scaling factor to approach the quality of computationally-demanding anharmonic frequencies. [179, 180]

When determining the relative populations of different states, usually chemically very similar structures are compared, e.g. two transition states leading to different regioisomers. A substantial cancellation of errors may be expected and therefore the accuracy of the result is beyond the accuracy of the method in many cases. On the other hand, one should keep in mind that TST is a classical theory which neglects quantum and dynamic effects. Common examples of these are tunneling [181,182] and bifurcation [183], where one transition state leads to at least two products.

2.10 Molecular properties

The previous discussion has focused on computing the wave function and the energy of the system. Once they are available, many interesting properties can be computed. In this work, we have used partial charges and computed NMR chemical shifts to understand reactivity and selectivity in chemical reactions.

2.10.1 Partial charges

Partial charges are not a measurable quantity and therefore they cannot be compared directly to the experimental values. They can, nevertheless, be com-

puted quantum chemically, and we found them to be extremely useful in order to explain the regioselectivity of the Pauson-Khand reaction.

The partial charge (q) of atom i in a molecule is defined as [5]:

$$q_i = Z_i - N(i), \tag{2.19}$$

where Z_i is the atomic number of atom i, and $N(i)$ is number of electrons associated with atom i in the molecule. The $N(i)$ can be computed based on orbital population or spatial electron distribution.

From orbital population methods, the earliest and very widely used method is the Mulliken population analysis, [184] which carries out a simple partitioning of the product of the bond orders and charges matrix and the atomic orbital basis function overlap matrix. This is a problem e.g. with diffuse atomic orbitals as the electrons might be actually closer to the next atom rather than the atom on which the orbital is centered. Therefore the Mulliken charges can change significantly according to the basis set.

In this work, we have frequently employed charges obtained from natural population analysis (NPA), also called natural bonding orbital (NBO) charges. [185, 186] In these, the $N(i)$ are evaluated by forming a set of natural atomic orbitals (NAO). As a consequence, they are more expensive to compute than Mulliken charges, but suffer from fewer problems. Hirshfeld charges have also been used in this work to confirm the conclusions based on NBO charges. [187] With Hirshfeld charges, the $N(i)$ is based on volume integration of the actual molecular electron density and a reference set of spherically-averaged atomic densities, instead of orbital populations.

2.10.2 NMR chemical shifts

Computed NMR chemical shifts can be very useful for the organic chemist to analyze complex experimental spectra. [188, 189] In order to compute NMR chemical shifts, the interaction of the molecular Hamiltonian with an external magnetic field has to be computed. The magnetic properties of the system should be independent of the origin of magnetic field vector, the so-called gauge origin; but this only holds when an infinite basis set is used. In practical computations, a finite basis set is employed and therefore the gauge origin has to be chosen. [190] In this work, two gauge origins have been employed: *individual gauge for localized orbitals* (IGLO) [191, 192] and *gauge-including atomic orbitals* (GIAOs) [193–195]. For practical aspects and recommendations on how to compute NMR shifts, Tantillo has recently published an excellent review. [196]

3 Results

The results of this work are published in four separate peer-reviewed articles, listed on page ii. The contributions of the authors in each article are explained on page iv. All articles are found as attachments in the Appendix, and here only a short summary of the central results is given. The Supplementary Information of papers II and IV included important parts of the work, and those are included in the Appendix (IIb and IVb). We also performed a small benchmark study to discover a suitable DFT method for homogeneous gold catalysis. This data is not included in the original articles and is discussed here. All computations have been performed employing a suitable RI-approximation as implemented in Turbomole [197] or Orca [198] program packages, and the prefix RI is omitted in the following discussion.

3.1 Benchmark study for gold complexes

Faza et al. [199] recently benchmarked 32 DFT functionals for homogeneous gold catalysis in order to choose the optimal one for reaction mechanism studies. The complexes were optimized at the CCSD/def2-SVP level and the energies were defined with higher level basis sets, def2-TZVPP. The problem is, however, that a double-ζ quality basis set is too small for electron correlation treatment in order to obtain sufficient geometries. This was highlighted in study by Nava et al. [200], where the geometries and the complexation energies were compared for four Au(I)-complexes (Fig. 3.1). Compared to high level CCSD(T)/def2-QZVPP reference calculations, the benchmark level used by Faza et al. was actually outperformed by all density functionals included in the study. The authors recommended the use of BP86 and TPSS functionals.

The inability of common density functionals to treat medium and long range correlation effects correctly, i.e. dispersion interactions, was discussed in Chapter 2. In this work, the dispersion forces have been treated using the atom pairwise corrected DFT-D3. The D3-correction was not included in the study of Nava et al., and therefore we decided to expand the study slightly to D3-corrected functionals with zero and BJ-damping, referred to as D3 and

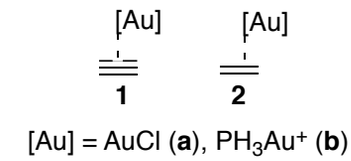

Fig. 3.1 The gold complexes chosen for the benchmark study.

D3BJ. Later, the recently published DLPNO-CCSD(T) method was included in the study. The def2-TZVPP basis set was used in all DFT computations and the relativistic effects for gold were treated with the RECP included in the basis set, in accordance with the reference level used by Nava et al. Accounting for scalar relativistic effects using the ZORA Hamiltonian was tested, and it was found to have a negligible effect on complexation energies. The DLPNO-CCSD(T) results were obtained using the ZORA Hamiltonian and the def2-TZVPP-ZORA basis set.

The results are summarized in Fig. 3.2. The mean absolute deviations (MAD) in the bond lengths are defined from the Au-L, C-C and both Au-C distances. The complexation energies are defined as E(**1**/**2**) - E(ethene/ethyne) - E(AuL), where AuL is AuCl (**a**) or $[AuPH_3]^+$ (**b**).

All density functionals tested provide accurate geometries for the restricted set of complexes. The D3-corrected TPSS is slightly better than without D3-corrections, with MAD less than 1 pm. The hybrid variant, TPSSh-D3, has the best performance for geometries. The BJ-damped D3 (D3BJ) provides worse results than zero damped in combination with the all studied functionals.

The complexation energies are overestimated by all functionals, and the effect is the most pronounced with the D3BJ-correction. However, the effect is very systematic and the result of both Au-complexes preferring coordination to ethene over ethyne is qualitatively correct with all functionals. On the other hand, for comparing small ligand effects, DFT might not be accurate enough:

- All methods provide a qualitatively correct answer to the question 'Is coordination preferred to alkenes over alkynes?'. The ΔE(**1**-**2**) values for AuCl and $[H_3PAu]^+$ are 5.0 and 4.3 kcal/mol at the reference level, respectively. The DFT methods estimate values between 2.9 and 4.0 kcal/mol, providing a qualitatively correct answer to the question.

- If the question was changed to 'How does the ligand affect the coordination energies?', then the DFT methods tested here might not be suitable. For this, we need to look at the ΔE(**1**-**2**)(**a**) - ΔE(**1**-**2**)(**b**) value. At the reference level, this is 0.7 kcal/mol (5.0 - 4.3 kcal/mol), suggesting that AuCl (**a**) prefers coordination to alkenes over alkynes slightly more than

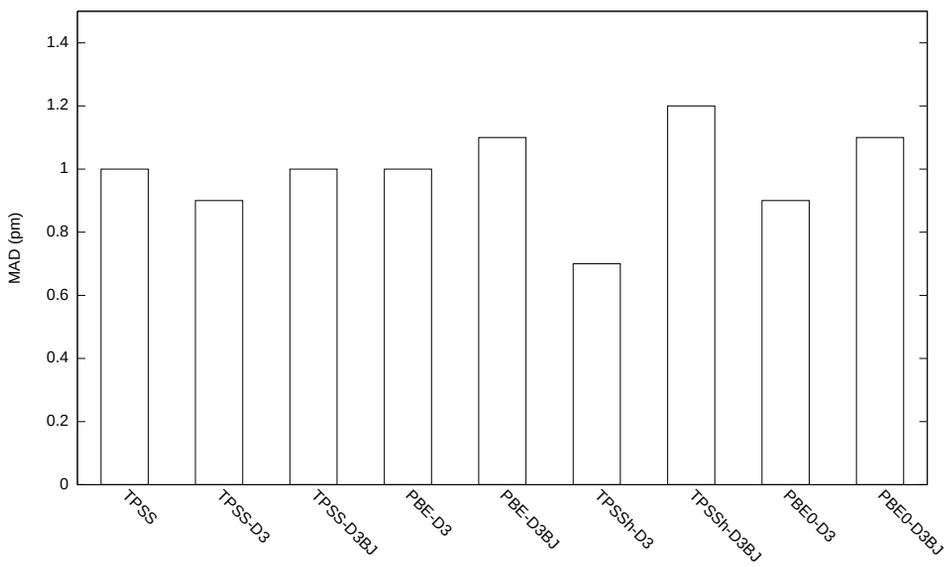

(a)

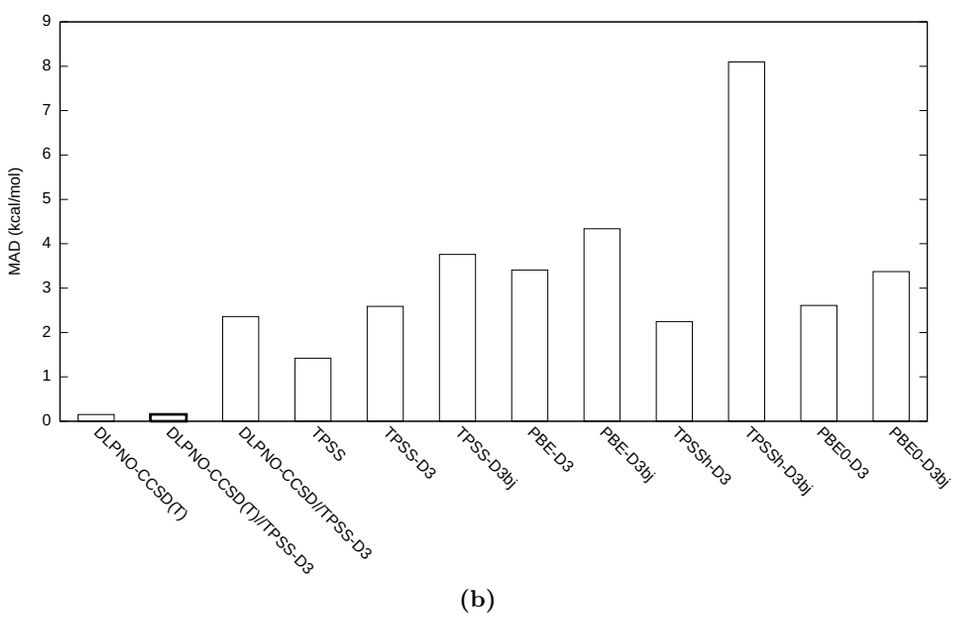

(b)

Fig. 3.2 The mean absolute deviations (MAD) in a) bond lengths and b) complexation energies compared to the CCSD(T)/def2-QZVPP reference for complexes **1a**/**b** and **2a**/**b**.

$[H_3PAu]^+$ (**b**). Density functionals provide values between 0.1 and 0.3 kcal/mol, estimating the ligand effect to be similar in both cases. Therefore, comparison of such small energy differences should be considered with caution.

The DLPNO-CCSD(T) method was released in autumn 2013 and therefore was not used originally in this work. It has been used later to recalculate some of the results. Here it was used for single-point energies for the reference and the TPSS-D3 structures. In complexation energies, MAD of only 0.1 kcal/mol is found when using either set of structures. The results are also consistent for the ligand effects, and therefore the DLPNO-CCSD(T) method can be considered as very promising for single point energies. The DLPNO-CCSD method does not provide a substantial improvement over DFT for complexation energies.

Based on the discussion above, the TPSS-D3 method was chosen for studying reactions involving gold. Geometries are slightly better with the hybrid variant TPSSh-D3, but the computational cost is also increased. Even though the TPSS functional provides slightly better complexation energies than TPSS-D3, we consider the D3-correction to be essential for the systems of interest. When computationally feasible, a heavily polarized def2-TZVPP basis set was selected. Otherwise, the slightly less polarized def2-TZVP basis set was employed.

3.2 Development of the Au(III) catalyst

During the past decade, cationic Au(I) complexes bearing N-heterocyclic (NHC) carbene or phosphine ligands have received an enormous amount of attention among many research groups. [201, 202] Due to the scalar relativistic contraction of the 6s and expansion of the 5d-orbitals, gold is the most electronegative transition metal. This makes it an efficient Lewis-acid for activating π-systems, such as alkynes. [203–205] A generally accepted simplified catalytic cycle for the activation of alkynes towards nucleophilic attack is shown in Scheme 3.1. The activated π-system **4** is electron deficient, and can react with various nucleophiles. In the formed vinyl-gold complex **5**, the gold and the nucleophile are typically *trans* to each other. In general, the nucleophilic attack is correctly predicted by Markovnikov's rule, but recent examples of Anti-Markovnikov additions exist. [206] The last step in the simplified catalytic cycle is the replacement of the gold with an electrophile (**5** $\rightarrow$ **6**). The electrophile is commonly a proton and this step is called protodeauration.

The catalytically active gold complex **3** can be either neutral or ionic (Scheme 3.2). Typical examples of neutral gold complexes are AuCl and $AuCl_3$,

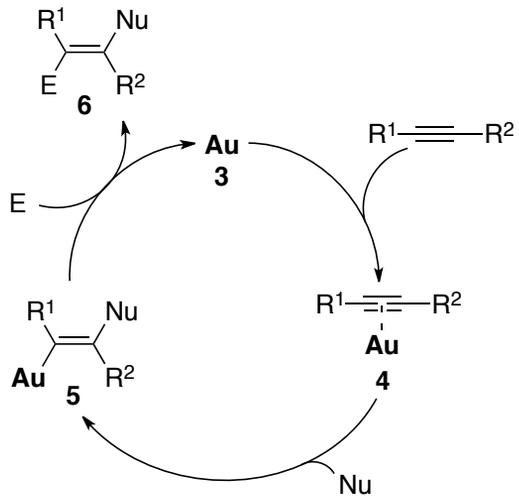

Scheme 3.1 A simplified catalytic cycle to elucidate the role of gold as a Lewis-acid.

both having a free low-lying unoccupied orbital to activate π-systems. The strong Lewis acidity of the simple Au(III) salt $AuCl_3$ has been known for a long time, e.g. Kharasch and Isbell noted in 1931 that it reacted rapidly with benzene. [207] In modern applications, the simple salts are commonly replaced by phosphine or NHC -liganded two-coordinated LAuCl or four-coordinated $LAuCl_3$ complexes, allowing fine tuning of the catalytic properties. [208] The liganded complexes do not have any low-lying free orbitals to activate π-systems, and π-systems are not capable of replacing the Au-Cl bond. Oxidative additions are also uncommon in general gold chemistry. [209] Therefore, a vacant coordination site is produced with a co-catalyst which is typically a Ag(I)-salt AgY, where Y is a weakly or non-coordinative counter ion, e.g. $^{-}NTf_2$ or ^{-}OTf. The use of silver as a co-catalyst is not only an additional cost, but also a possible source of crucial impurities. [210]

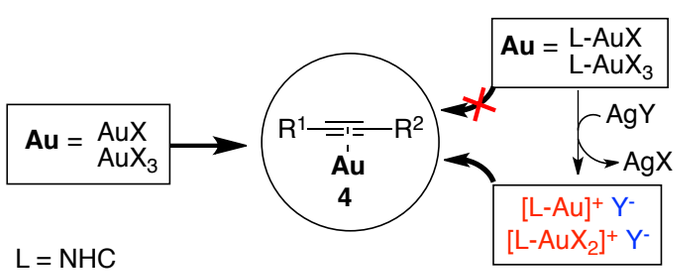

Scheme 3.2 Activation of alkynes with neutral and ionic gold-complexes.

In paper I an additive-free cationic Au(III) catalyst was designed and prepared. The hypothesis of the catalytically active species was supported by a

combination of experimental and computational studies. The catalyst is based on a pyridine side arm, which acts as a nucleophile on the gold center to generate an ionic and catalytically active species in the course of the reaction (Scheme 3.3). The π-systems are not able to replace the Au-Cl bond, but replacements of the Au-N bonds are known. [211] The concept is only possible for Au(III) due to the need for a square planar geometry.

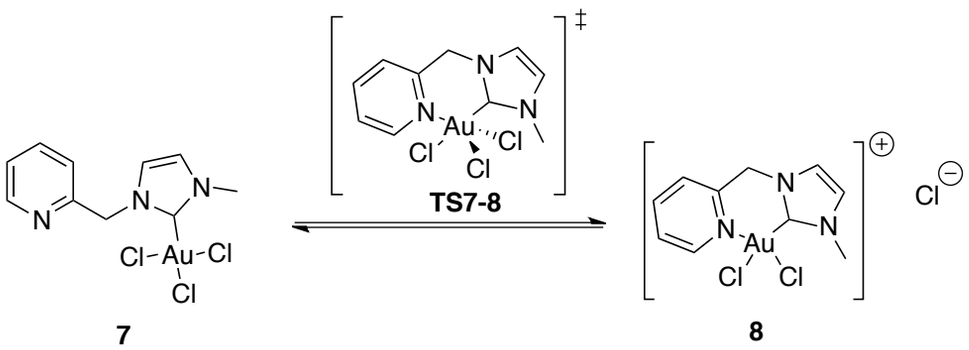

Scheme 3.3 Formation of the active catalyst **8**.

Three NHC-Au(III) complexes **A**-**C** (Fig. 3.3) were prepared and studied both, experimentally and computationally. The catalytic activities of the complexes were tested in two alkyne activation reactions, showing **B** to be more active than **A**. The correlation of the nucleophilic properties of the pyridine with the catalytic activity supports our initial hypothesis on pyridine acting as a nucleophile. The complex **C** was synthesized as a reference catalyst, having similar electronic properties to **A** and **B**, but lacking the possibility of nucleophilic attack. As expected, no activity was observed for complex **C**.

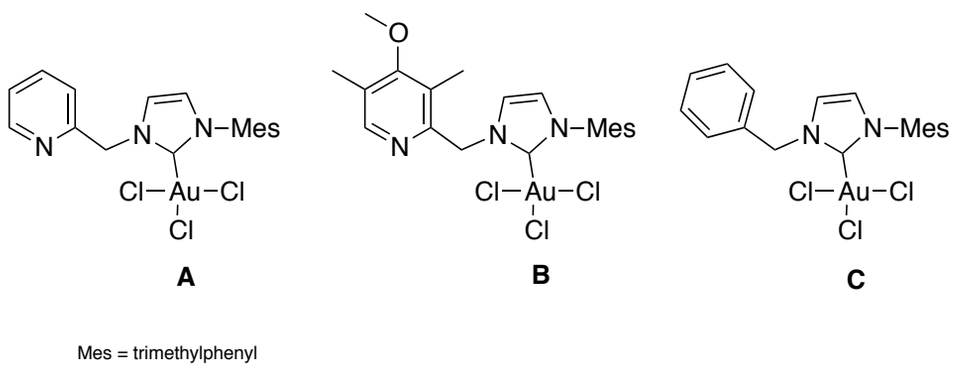

Fig. 3.3 Synthesized Au(III)-NHC complexes in Paper I.

3.2.1 Further studies

Complex **B** was found to be an effective catalyst in the cycloisomerization of alkynylfuran **9** to isobenzofuranol **10** (Scheme 3.4), as discussed in the paper. This reaction was also used in further studies to probe the reactivity. Another test reaction used in Paper I, involving an activation of *o*-alkynylaniline, may be problematic due to gold thermodynamically favoring coordination to the amine over the alkyne, [212] as noted in our separate study so this was not considered further.

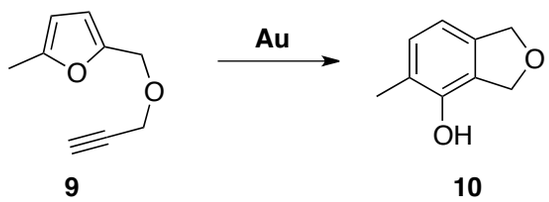

Scheme 3.4 The reaction used to benchmark the catalytic activity of complexes **A**-**C**.

During the initial work, the catalyst **B** was found to be operative in chloroform ($CHCl_3$), whereas no activity was observed in acetonitrile (MeCN) at ambient temperatures. Later, the turnover number (TON) of complex **B** was improved slightly when changing the solvent to dichloromethane (DCM). The reaction was originally reported in MeCN, [213] and therefore we consider the solvent effect to be related to the generation of the active species rather than the overall catalytic cycle.

The possible coordination of MeCN to the gold might slow down the catalytic cycle, but it should not inhibit it completely. This was confirmed in experiments, where the reaction had been completely inactive in MeCN for hours until it was initiated by the addition of a small amount of DCM into the solution. We consider the solvent effect to be related to the ability of the solvent to stabilize the chloride anion by hydrogen bonding as discussed below.

The transformation of the neutral state **7** to the presumed catalytically active ionic state **8** was studied computationally in order to understand the effect (Fig. 3.4). A slightly reduced model system, where the mesitylene-group is changed to a methyl-group according to Scheme 3.3 was used. All structures were optimized using the TPSS-D3/def2-TZVP method in DCM and MeCN, treating the solvent effects with the COSMO model. The results are tabulated in Table 3.1.

In the COSMO model, the solvents differ from each other only by their dielectric constants, which are 8.9 and 37.5 for DCM and MeCN, respectively. [214] In order to include a more realistic description of hydrogen bonding of

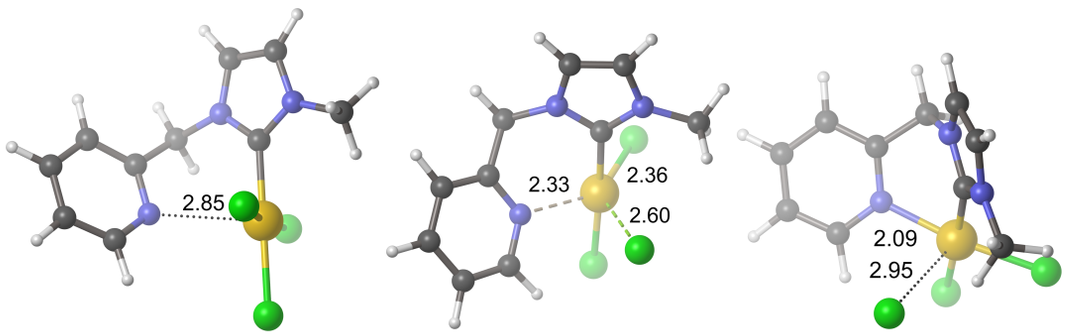

(a) 7 **(b) TS7-8** **(c) 8**

Fig. 3.4 Visualization of the neutral (**7**), transition (**TS7-8**) and ionic (**8**) states of model system, optimized at TPSS-D3/def2-TZVP level in DCM (COSMO).

the solvent, the COSMO model for real solvents (COSMO-RS) was used for solvation energies for the COSMO optimized structures. The experimental results indicate the ionic state to be more stabilized in DCM than in MeCN. As expected, the COSMO model gives results *vice versa* which is easy to understand as the MeCN is more polar, i.e. it has higher dielectric constant. When taking the hydrogen-bonding ability of the solvent into account with COSMO-RS, the ionic state is more stabilized in DCM than in MeCN.

Table 3.1 The ΔG(298K) values for **7**,**8** and **TS7-8**.

Method	**Solvent**	**Model**	**7**	**TS7-8**	**8**
CCSD(T)	DCM	COSMO	0	13.7	6.5
TPSS-D3	DCM	COSMO	0	9.1	5.2
TPSS-D3	MeCN	COSMO	0	8	2.9
TPSS-D3	DCM	COSMO-RS	0	-	4.8
TPSS-D3	MeCN	COSMO-RS	0	-	5.8

It seems that the hydrogen bonding ability of the solvent is crucial in order for complexes **A** and **B** to reach their catalytically active ionic states. To confirm the hypothesis, trifluoroethanol (TFE) was used as solvent, being a strong H-bond donor but a weak acceptor. The catalysts were found to be active, and TFE was also observed to boost the reaction in MeCN similarly to DCM. The optimal solvent for the catalyst was still found to be DCM, but the success of the experiment provides additional support for the hypothesis.

Single-point energies for all three structures were also calculated using the DLPNO-CCSD(T)/def2-TZVPP-ZORA method. The SIE of DFT is seen in the underestimation of the activation energy barrier by several kcal/mol, but the ΔG value is well estimated. Differences according to the solvents are noted to be reliable already at the TPSS-D3 level.

3.3 Au(III) - Aspects of the reaction mechanism

In Paper II the reaction mechanism for Au(III) catalyzed conversion of chiral enyneamine **11** to chiral cyclopentadiene **12** was studied (Scheme 3.5). The proposed catalytic cycle, involving a dual Au(III)-assisted *cis-trans* -isomerization, was concluded from a combination of experimental and computational studies.

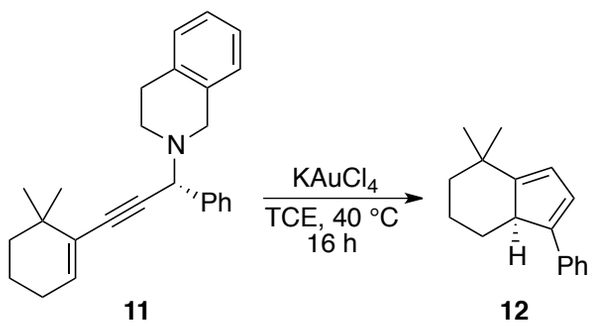

Scheme 3.5 Au(III)-catalyzed synthesis of chiral cyclopentadienes.

According to the previously discussed benchmark results, TPSS-D3/def2-TZVP was chosen as the computational method. The cyclization step, which determines the enantioselectivity, was studied using a wider variety of density functionals, all giving a very good correlation with the experiment. A direct *cis-trans* -isomerization of vinyl-Au(III) species **13-*cis*** was noted to require treatment of static correlation and therefore the NEVPT2 method was applied (Scheme 3.6). Comparison of the performance of different functionals on the enantioselectivity, and an extensive study on how static correlation was treated, have been published in the Supplementary Information of the original article, and are included in the appendix (IIb).

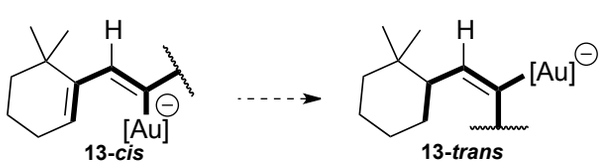

Scheme 3.6

An additional interesting aspect related to *cis-trans* -isomerization is the gold-carbene behaviour. This discussion was started by Toste and coworkers [215] and continued by several authors as discussed in the paper. Vinyl Au(I) and Au(III) are able to stabilize carbocations by back-donating electrons from their filled 5*d*-shells, as elucidated in Scheme 3.7. The carbocation **14a** is

mainly considered to be stabilized by the carbenoid structure **14b**, whereas the lifetime of the true gold-carbene **14c** is short, if it exists at all. [216]. In accordance with this, we observed a carbenoid-type structure to be dominant in the ground states, but considered that the carbene reactivity may be operative in the transition states.

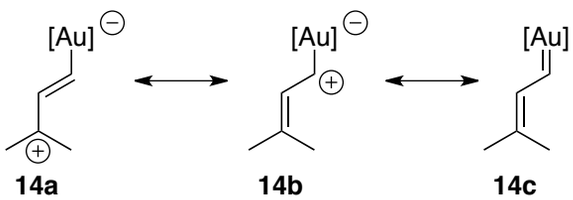

Scheme 3.7 The gold-carbene behaviour.

3.4 Regioselectivity in the Pauson-Khand reaction

The Pauson-Khand (PK) reaction is a cobalt-mediated [2+2+1] cycloaddition between alkyne, alkene and carbon monoxide (Scheme 3.8). [217–220] The alkyne and alkene can be present in the same molecule or in two separated molecules, providing respective intra- and intermolecular versions of the reaction. Our study and the concomitant discussion are restricted to the latter.

When unsymmetrical alkynes ($R^1 \neq R^2$) are used, two regioisomers may be formed. These are typically named as α- and β-regioisomers, defined by the relative position of the substituent compared to the carbonyl carbon. For example, **17** is the α- and **18** is the β-regioisomer according to R^1. Different substituents polarize the alkyne differently, and in papers III and IV we have studied how this affects the regioselectivity of the PK-reaction. Our aim was not only to understand the factors affecting the selectivity, but also to provide simple tools to predict it.

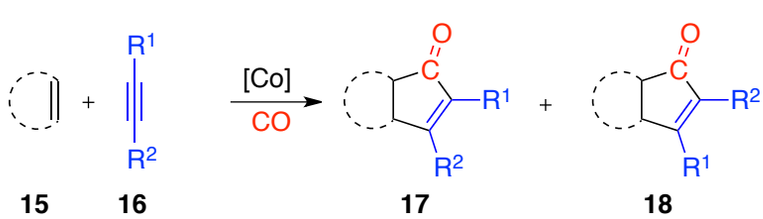

Scheme 3.8 The Pauson-Khand reaction.

The reactivity of the Pauson-Khand reaction is dependent on the nature of the olefin. [221] Here, the alkenes were restricted to norbornene and norbornediene, where the former has been shown to be slightly less regioselective

in the PK reaction than the latter. [222] While the PK-reaction is known to provide regioselective building blocks for complex molecules, [223, 224] the use of norbornediene as alkene may serve as a platform to provide an efficient route to both regioselective and enantioselective cyclopentenones: The PK-product **20** can undergo a retro-Diels-Alder reaction and can be obtained by an enantioselective PK-reaction (Scheme 3.9). [225, 226] Therefore, understanding the factors affecting the regioselectivity are of essential interest.

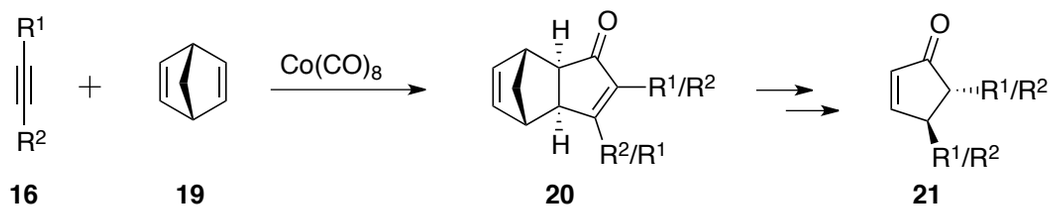

Scheme 3.9

3.4.1 The reaction mechanism

The key steps of the mechanism, shown in Scheme 3.10, are well-established. [227, 228] First, the alkyne **16** reacts with $Co_2(CO)_8$ to form a dicobalthexacarbonyl-complex **22**. With loss of one CO ligand, the pentacarbonyl-complex is able to coordinate to an alkene (**23**). The next step, the insertion of the alkene into the alkyne (**23** → **24**), determines the regioselectivity and is considered to be non-reversible. [228] The last steps in formation of the cyclopentenone **26** are the insertion of CO into the cobaltocycle (**24** → **25**) and the reductive elimination and dissociation of the dicobalt unit.

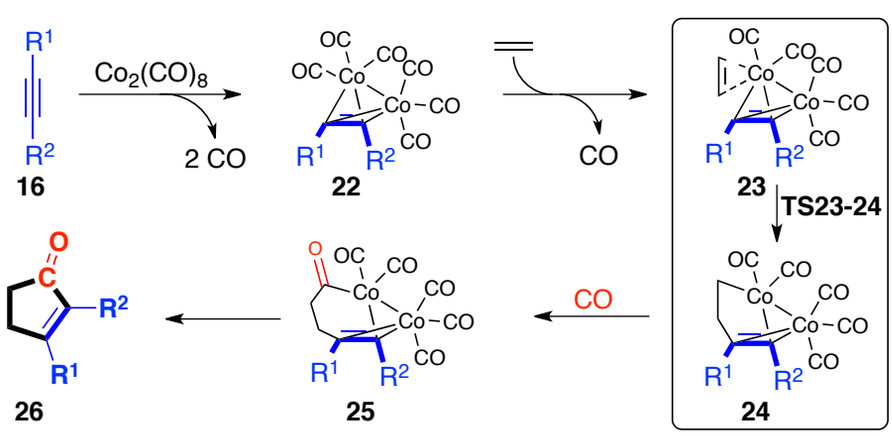

Scheme 3.10 The key steps of the PK reaction mechanism.

The alkene can be accommodated in either an equatorial or axial position

in the complex **23** (Fig. 3.5), resulting in a number of transition states leading to α- or β-regioisomers. However, the energy barrier for the alkene to pseudorotate between the coordination sites has been shown to be low compared to the energy required for the insertion, [229] so the initial C-C bond is preferably formed in the axial position. [229, 230] Our findings for norbornediene are in accordance with these results, and are found in the Supplementary Information of Paper IV (IVb in the appendix).

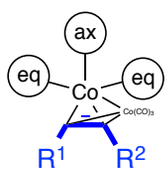

Fig. 3.5 Nomenclature of the coordination sites: ax = axial; eq = equatorial.

3.4.2 Factors determining regioselectivity

A model for the transition state is shown in Fig. 3.6. The substituent attached to the alkynyl carbon where the initial C-C bond is formed occupies the β -position in the final product. The α : β regioselectivity is affected by the steric and electronic nature of the substituents. Electron withdrawing groups (EWG) have been shown to favour the β-position and electron donating (EDG) groups favour the α-position. [231–233] This is considered to be controlled by the alkyne polarization where the initial C-C -bond is formed to the more electron rich alkynyl carbon. [230] The steric effects override the electronic effects, probably by sterically hindering the required transition state. [234,235]

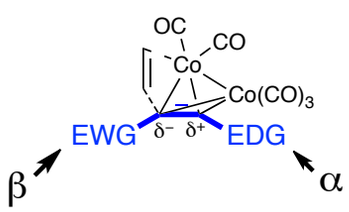

Fig. 3.6 A model of the transition state where the initial C-C -bond is formed.

The first strong argument in the alkyne polarization induced regioguidance is based on the experiment of Milet and Greene, who noted that the diarylalkyne **27** only gave the pure isomer **28** having the EWG-group in the β-position (Scheme 3.11). [233] Here the selectivity can be considered to arise from the electronic effects, as the EDG/EWG functional groups are placed

quite distant from the reaction center in order to neglect the steric effects. However, the experimental discovery in paper III suggested an error in the corresponding characterization where the **28**/**29**-ratio was re-determined to be 1.3/1 instead of 1/0. In papers III and IV, our aim has been to provide a realistic picture of electronic regioguidance in the PK-reaction.

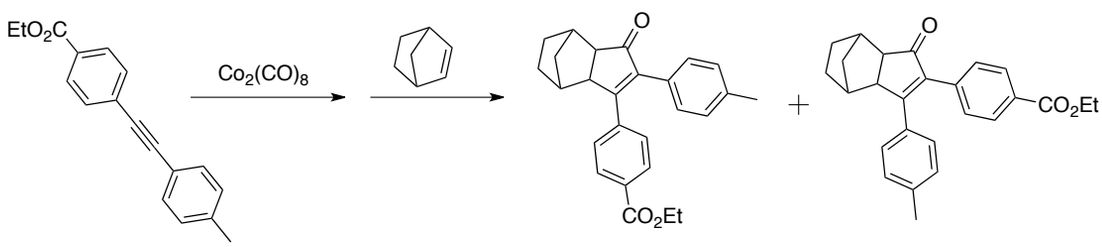

Scheme 3.11

3.4.3 Alkyne polarization

The alkyne polarization can be considered to be mediated by resonance and inductive effects. In paper III we studied a set of diarylalkynes which were substituted with different EDG/EWG groups at *ortho* and *para* positions (Scheme 3.11). Here, the alkyne polarization was mainly due to the resonance effect. In paper IV the study was restricted to the inductive effect by studying aliphatic alkynes instead of conjugated diarylalkynes (Scheme 3.12)

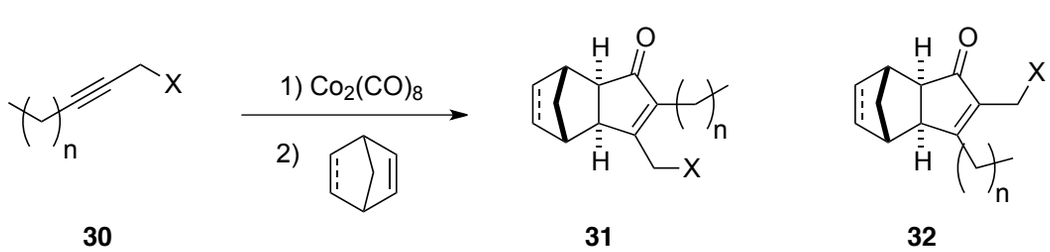

Scheme 3.12

In the case of aliphatic alkynes, the polarization of the alkyl carbons dictates the regioselectivity and a qualitative correlation can be found between the regioselectivity and the NBO charges of the alkynyl carbons, which is in accordance with the previously published model. [230] However, this does not always hold for diarylalkynes. For instance, the NBO charges and the experimental results for three methoxy substituted diarylalkynes are shown in Fig. 3.7. The α/β-ratio is changed from 1.6/1 to 1/1.6 when the substitution

is changed from the *para*-position (**33**) to both *ortho*-positions (**35**). When all three positions were substituted (**34**), an α/β-ratio of 1/1.4 was obtained.

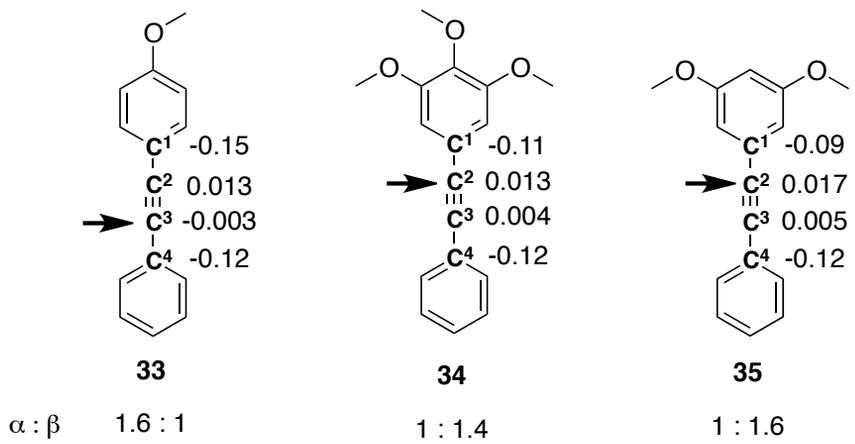

Fig. 3.7 The computed NBO charges at TPSS-D3/def2-TZVPP level for **33**-**35**. The black arrow points to the carbon where the C-C bond formation is experimentally preferred.

The black arrow points to the alkynyl carbon where initial C-C bond formation is preferred, according to the experimental data. This is the more electron rich carbon only in the case of **33**. Therefore, this model provides a qualitatively incorrect prediction of the regioselectivity for substrates **34** and **35**. To understand why the polarization is not visible in the alkynyl carbons, electron density difference plots of **33** and **35** are shown in Fig. 3.8. These plots are made by subtracting the electron density of the substituted diarylalkyne from the non-substituted diarylalkyne. The blue color indicates increased electron density and the red colour reduced electron density. Large areas of increased electron density can be seen where the methoxy groups are introduced, but the focus is on the polarization of the phenyl ring and the alkynyl carbons.

Resonance effect mediated *ortho*/*para*-directed polarization is clearly seen for the both substrates. However, for **35** the polarization effect is no longer visible in the alkynyl carbons. In both cases, a clear polarization can be seen in the carbon bonded to the alkynyl carbon. We consider that this polarization will act as EWG/EDG in the course of the reaction and therefore dictate the regioselectivity. Indeed, the regioselectivity for all studied substrates correlates qualitatively, and in certain limits even quantitatively, with the computed NBO charges of the C^1 and C^4 -positions (Fig. 3.7).

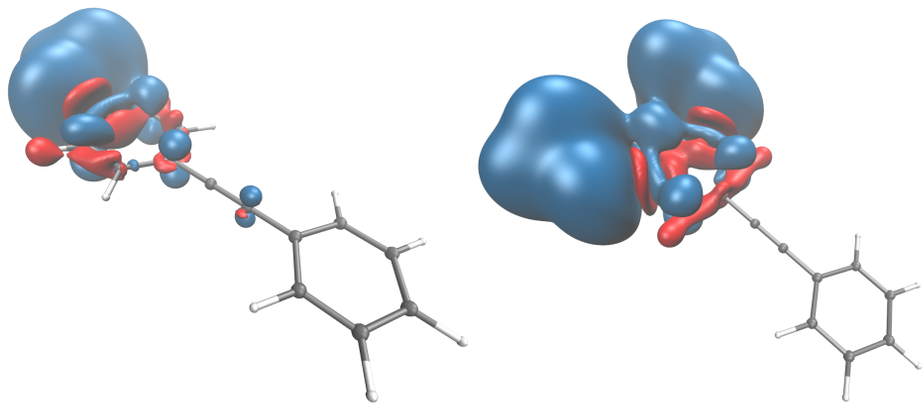

(a) 33 **(b) 35**

Fig. 3.8 The relative electron densities for substrates **33** and **35** compared to the electron density of 1,2-diphenylethyne. Blue and red colors indicate increased and reduced electron density, respectively. Isosurfaces are plotted using isovalue of ±0.001.

3.4.4 Weak interactions

In paper IV we also wanted to understand other factors affecting the regioselectivity in addition to the electronic factors. This was done by studying three model systems where the effects of the substituent were compared to the methyl group as explained in the paper. With these model systems, we could elucidate how the steric effects override even very large electronic effects of the CF_3 -group, and discovered interesting aspects concerning how intramolecular hydrogen bonding can affect the regioselectivity (Scheme 3.13). It seems that intramolecular hydrogen bonding between the alkyne substituents and H^4 has a notable effect on the regioselectivity. The hydrogen bond makes the hydrogen slightly more acidic, which was shown to facilitate the reaction. It can be considered that the hydrogen bond allows donation of electron density of the C-H^4 bond to the C-C bond formation, and therefore lowers the activation energy barrier.

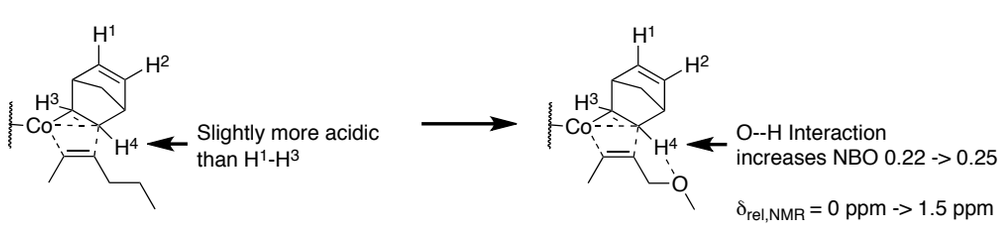

Scheme 3.13

3.4.5 Computational methods and accuracy

In addition to gold-complexes, TPSS(-D3) functional has also been shown to describe other transition metal complexes very well. [133, 236, 237] Therefore, the study has been performed mainly at the TPSS-D3/def2-TZVPP (alkynes) or TPSS-D3/def2-TZVP (dicobalt complexes) levels. In the course of the study, the results have been reliably confirmed using other density functionals and the alkyne polarizations were also confirmed at the MP2/def2-QZVPP level. The use of HF-based wave-function methods for dicobalt complexes may, nevertheless, be problematic due to spin-contamination, whereas non-hybrid DFT was found to reproduce CASPT2 electronic structure results. [238]

The assumed non-reversibility of the alkene-insertion step means that the regioselectivity is kinetically controlled. According to the TST, the α/β-ratio is determined as the difference between the activation energies to reach **TS23-24** for α- and β-regioisomers from **23**. Due to pseudorotation, a comprehensive ground state study can be neglected, as we can assume all transition states to rise from the same global minimum. The regioselectivity should therefore be defined as the direct energy difference between the transition states. Computationally this means that the energy differences are compared between chemically similar conformers, and therefore DFT-D3 computations should be accurate for the transition state comparison in paper IV. The results were also confirmed using several other density functionals and also with larger basis sets. This data is found in the Supplementary Information of paper IV, and is included in the appendix (IVb).

Alkyne polarization was studied using NBO charge analysis. The charge differences are very small and therefore the results in paper III were also confirmed as reliable compared to the Hirshfeld charges. The NMR-computations in paper IV were confirmed to be reliable by using two approaches: GIAO-/BP86/def2-TZVPP and IGLO/TPSSh/def2-TZVPP.

4 Conclusions

Quantum chemistry can be a powerful methodology for a chemist to provide an understanding of complex chemical systems. In this work, it has been used in combination with experimental studies to understand factors affecting the selectivity in chemical reactions or activity of a catalyst. The collaboration of both fields has been essential, and the results presented here would not have been possible without it. The most important results of this work can be separated as follows.

- New types of Au(III)-catalysts were designed and prepared. The benefit of these catalysts is that they are able to activate π-systems without any co-catalyst, unlike traditionally used liganded Au(I)/Au(III) complexes. The co-catalyst is not only an additional cost but also a potential source of impurities, which might be crucial e.g. in medicinal chemistry applications. The combination of computational and experimental studies provided us with an understanding of how the catalysts work, and this has started a line of research which is ongoing in our laboratory.

- In addition to catalyst design, the mechanistic understanding of transition metal catalysts is of significant importance. The simple Au(III) salt $AuCl_3$ is known to be an efficient Lewis-acid for activating π-systems. We discovered a potential role for $AuCl_3$ to act as both a Lewis acid and Lewis base in *cis-trans* isomerization of vinyl-gold species. This may influence further studies when reactions involving gold complexes are considered.

- Apart from Au(III)-chemistry, computational methods were applied in order to understand the regioselectivity of the Pauson-Khand reaction. We were able to design a simple computational model which was able to provide a qualitative, and within certain limits even quantitative, prediction of the regiochemical distribution of the products. The model is based on NBO charges that are simple to compute. Moreover, it was found that intramolecular hydrogen bonds can affect the regioselectivity of the reaction. We hope that these findings may assist synthetic chemists in order

to predict regiochemical outcomes of the Pauson-Khand reaction.

Bibliography

[1] G. Wang, M. Zhou, J. T. Goettel, G. J. Schrobilgen, J. Su, J. Li, T. Schloder, S. Riedel. Identification of an iridium-containing compound with a formal oxidation state of IX. *Nature* **2014**, *514*, 475–477.

[2] H. S. Rzepa. Can 1,3-dimethylcyclobutadiene and carbon dioxide coexist inside a supramolecular cavity? *Chemical Communications* **2011**, *47*, 1851–1853.

[3] P. Pyykkö, N. Runeberg. Icosahedral WAu12: A Predicted Closed-Shell Species, Stabilized by Aurophilic Attraction and Relativity and in Accord with the 18-Electron Rule. *Angewandte Chemie International Edition* **2002**, *41*, 2174–2176.

[4] X. Li, B. Kiran, J. Li, H.-J. Zhai, L.-S. Wang. Experimental Observation and Confirmation of Icosahedral W@Au12 and Mo@Au12 Molecules. *Angewandte Chemie International Edition* **2002**, *41*, 4786–4789.

[5] S. Bachrach, *Computational Organic Chemistry 2nd ed.*, John Wiley and Sons, **2014**.

[6] F. Jensen, *Introduction to Computational Chemistry 2nd ed.*, John Wiley and Sons, **2007**.

[7] B. Radovan, P. Widmark (Eds.), *European Summerschool in Quantum Chemistry 2013, Book I*, ESQC Committee, **2013**.

[8] B. Radovan, P. Widmark (Eds.), *European Summerschool in Quantum Chemistry 2013, Book II*, ESQC Committee, **2013**.

[9] B. Radovan, P. Widmark (Eds.), *European Summerschool in Quantum Chemistry 2013, Book III*, ESQC Committee, **2013**.

[10] J. Goodman, *Chemical Applications of Molecular Modelling*, Royal Society of Chemistry, **1998**.

[11] R. J. Bartlett. Many-Body Perturbation Theory and Coupled Cluster Theory for Electron Correlation in Molecules. *Annual Review of Physical Chemistry* **1981**, *32*, 359–401.

[12] O. Vahtras, J. Almlöf, M. Feyereisen. Integral approximations for LCAO-SCF calculations. *Chemical Physics Letters* **1993**, *213*, 514 – 518.

[13] M. Feyereisen, G. Fitzgerald, A. Komornicki. Use of approximate integrals in ab initio theory. An application in MP2 energy calculations. *Chemical Physics Letters* **1993**, *208*, 359 – 363.

[14] K. Eichkorn, O. Treutler, H. Öhm, M. Häser, R. Ahlrichs. Auxiliary basis sets to approximate Coulomb potentials. *Chemical Physics Letters* **1995**, *240*, 283 – 290.

[15] F. Weigend, M. Häser, H. Patzelt, R. Ahlrichs. RI-MP2: optimized auxiliary basis sets and demonstration of efficiency. *Chemical Physics Letters* **1998**, *294*, 143 – 152.

[16] F. Neese. An improvement of the resolution of the identity approximation for the formation of the Coulomb matrix. *Journal of Computational Chemistry* **2003**, *24*, 1740–1747.

[17] F. Neese, F. Wennmohs, A. Hansen, U. Becker. Efficient, approximate and parallel Hartree–Fock and hybrid DFT calculations. A 'chain-of-spheres' algorithm for the Hartree–Fock exchange. *Chemical Physics* **2009**, *356*, 98 – 109.

[18] S. Kossmann, F. Neese. Comparison of two efficient approximate Hartee–Fock approaches. *Chemical Physics Letters* **2009**, *481*, 240 – 243.

[19] P. Pyykkö. Relativistic effects in structural chemistry. *Chemical Reviews* **1988**, *88*, 563–594.

[20] P. Pyykkö. Relativistic Effects in Chemistry: More Common Than You Thought. *Annual Review of Physical Chemistry* **2012**, *63*, 45–64.

[21] M. Born, R. Oppenheimer. Zur Quantentheorie der Molekeln. *Annalen der Physik* **1927**, *389*, 457–484.

[22] I. Rahinov, R. Cooper, D. Matsiev, C. Bartels, D. J. Auerbach, A. M. Wodtke. Quantifying the breakdown of the Born-Oppenheimer approximation in surface chemistry. *Physical Chemistry Chemical Physics* **2011**, *13*, 12680–12692.

[23] S. Pisana, M. Lazzeri, C. Casiraghi, K. S. Novoselov, A. K. Geim, A. C. Ferrari, F. Mauri. Breakdown of the adiabatic Born-Oppenheimer approximation in graphene. *Nature Materials* **2007**, *6*, 198–201.

[24] E. Tapavicza, G. D. Bellchambers, J. C. Vincent, F. Furche. Ab initio non-adiabatic molecular dynamics. *Physical Chemistry Chemical Physics* **2013**, *15*, 18336–18348.

[25] M. S. Molloy, J. A. Snyder, A. E. Bragg. Structural and Solvent Control of Nonadiabatic Photochemical Bond Formation: Photocyclization of o-Terphenyl in Solution. *The Journal of Physical Chemistry A* **2014**, *118*, 3913–3925.

[26] D. R. Hartree. The wave mechanics of an atom with a non-Coulomb central field. Part I. Theory and methods. *Proceedings of the Cambridge Philosophical Society* **1928**, *24*, 89.

[27] D. R. Hartree. The wave mechanics of an atom with a non-Coulomb central field. Part II. Some results and discussions. *Proceedings of the Cambridge Philosophical Society* **1928**, *24*, 111.

[28] V. Fock. Näherungsmethode zur Lösung des quantenmechanischen mehrkörperproblems. *Zeitschrift fur Physik* **1930**, *61*, 126.

[29] R. S. Paton. Dissecting non-covalent interactions in oxazaborolidinium catalyzed cycloadditions of maleimides. *Organic and Biomolecular Chemistry* **2014**, *12*, 1717–1720.

[30] A. Armstrong, R. A. Boto, P. Dingwall, J. Contreras-Garcia, M. J. Harvey, N. J. Mason, H. S. Rzepa. The Houk-List transition states for organocatalytic mechanisms revisited. *Chemical Science* **2014**, *5*, 2057–2071.

[31] R. F. Frey, M. Cao, S. Q. Newton, L. Schäfer. Electron correlation effects in aliphatic non-bonded interactions: comparison of n-alkane MP2 and HF geometries. *Journal of Molecular Structure: THEOCHEM* **1993**, *285*, 99 – 113.

[32] S. Grimme. Seemingly Simple Stereoelectronic Effects in Alkane Isomers and the Implications for Kohn–Sham Density Functional Theory. *Angewandte Chemie International Edition* **2006**, *45*, 4460–4464.

[33] M. Wodrich, C. Wannere, Y. Mo, P. Jarowski, K. Houk, P. Schleyer. The Concept of Protobranching and Its Many Paradigm Shifting Implications for Energy Evaluations. *Chemistry – A European Journal* **2007**, *13*, 7731–7744.

[34] S. Grimme. n-Alkane Isodesmic Reaction Energy Errors in Density Functional Theory Are Due to Electron Correlation Effects. *Organic Letters* **2010**, *12*, 4670–4673.

[35] W. C. McKee, P. v. R. Schleyer. Correlation Effects on the Relative Stabilities of Alkanes. *Journal of the American Chemical Society* **2013**, *135*, 13008–13014.

[36] P. R. Schreiner, L. V. Chernish, P. A. Gunchenko, E. Y. Tikhonchuk, H. Hausmann, M. Serafin, S. Schlecht, J. E. P. Dahl, R. M. K. Carlson, A. A. Fokin. Overcoming lability of extremely long alkane carbon-carbon bonds through dispersion forces. *Nature* **2011**, *477*, 308–311.

[37] W. Thiel. Semiempirical quantum–chemical methods. *Wiley Interdisciplinary Reviews: Computational Molecular Science* **2014**, *4*, 145–157.

[38] S. Grimme, S. Ehrlich, L. Goerigk. Effect of the damping function in dispersion corrected density functional theory. *Journal of Computational Chemistry* **2011**, *32*, 1456–1465.

[39] R. Sure, S. Grimme. Corrected small basis set Hartree-Fock method for large systems. *Journal of Computational Chemistry* **2013**, *34*, 1672–1685.

[40] R. Sure, J. Antony, S. Grimme. Blind Prediction of Binding Affinities for Charged Supramolecular Host–Guest Systems: Achievements and Shortcomings of DFT-D3. *The Journal of Physical Chemistry B* **2014**, *118*, 3431–3440.

[41] C. W. Bauschlicher, P. Taylor. Full CI benchmark calculations for molecular properties. *Theoretica chimica acta* **1987**, *71*, 263–276.

[42] C. W. Bauschlicher, S. R. Langhoff. Full CI benchmark calculations on N2, NO, and O2: A comparison of methods for describing multiple bonds. *The Journal of Chemical Physics* **1987**, *86*, 5595–5599.

[43] M. Caffarel, E. Giner, A. Scemama, A. Ramírez-Solís. Spin Density Distribution in Open-Shell Transition Metal Systems: A Comparative Post-Hartree–Fock, Density Functional Theory, and Quantum Monte Carlo Study of the CuCl2 Molecule. *Journal of Chemical Theory and Computation* **2014**, *10*, 5286–5296.

[44] H. Larsen, J. Olsen, P. Jørgensen, O. Christiansen. Full configuration interaction benchmarking of coupled-cluster models for the lowest singlet energy surfaces of N2. *The Journal of Chemical Physics* **2000**, *113*, 6677–6686.

[45] P. Surján, *The Brillouin Theorem* in *Second Quantized Approach to Quantum Chemistry*, Springer Berlin Heidelberg, **1989**, pp. 87–92.

[46] C. Møller, M. Plesset. Note on an Approximation Treatment for Many-Electron Systems. *Physical Review* **1934**, *46*, 618–622.

[47] D. Cremer. Møller–Plesset perturbation theory: from small molecule methods to methods for thousands of atoms. *Wiley Interdisciplinary Reviews: Computational Molecular Science* **2011**, *1*, 509–530.

[48] B. Forsberg, Z. He, Y. He, D. Cremer. Convergence behavior of the Møller–Plesset perturbation series: Use of Feenberg scaling for the exclusion of backdoor intruder states. *International Journal of Quantum Chemistry* **2000**, *76*, 306–330.

[49] T. Risthaus, S. Grimme. Benchmarking of London Dispersion-Accounting Density Functional Theory Methods on Very Large Molecular Complexes. *Journal of Chemical Theory and Computation* **2013**, *9*, 1580–1591.

[50] S. Ehrlich, H. F. Bettinger, S. Grimme. Dispersion-Driven Conformational Isomerism in σ-Bonded Dimers of Larger Acenes. *Angewandte Chemie International Edition* **2013**, *52*, 10892–10895.

[51] E. G. Hohenstein, C. D. Sherrill. Wavefunction methods for noncovalent interactions. *Wiley Interdisciplinary Reviews: Computational Molecular Science* **2012**, *2*, 304–326.

[52] S. Grimme. Improved second-order Møller–Plesset perturbation theory by separate scaling of parallel- and antiparallel-spin pair correlation energies. *The Journal of Chemical Physics* **2003**, *118*, 9095–9102.

[53] S. Grimme, L. Goerigk, R. F. Fink. Spin-component-scaled electron correlation methods. *Wiley Interdisciplinary Reviews: Computational Molecular Science* **2012**, *2*, 886–906.

[54] L. Goerigk, S. Grimme. A thorough benchmark of density functional methods for general main group thermochemistry, kinetics, and noncovalent interactions. *Physical Chemistry Chemical Physics* **2011**, *13*, 6670–6688.

[55] I. Hyla-Kryspin, S. Grimme. Comprehensive Study of the Thermochemistry of First-Row Transition Metal Compounds by Spin Component Scaled MP2 and MP3 Methods. *Organometallics* **2004**, *23*, 5581–5592.

[56] J. Čížek. On the Correlation Problem in Atomic and Molecular Systems. Calculation of Wavefunction Components in Ursell-Type Expansion Using Quantum-Field Theoretical Methods. *The Journal of Chemical Physics* **1966**, *45*, 4256–4266.

[57] R. J. Bartlett. Coupled-cluster approach to molecular structure and spectra: a step toward predictive quantum chemistry. *The Journal of Physical Chemistry* **1989**, *93*, 1697–1708.

[58] J. Řezáč, P. Hobza. Describing Noncovalent Interactions beyond the Common Approximations: How Accurate Is the "Gold Standard," CCSD(T) at the Complete Basis Set Limit? *Journal of Chemical Theory and Computation* **2013**, *9*, 2151–2155.

[59] P. Pulay. Localizability of dynamic electron correlation. *Chemical Physics Letters* **1983**, *100*, 151–154.

[60] S. Sæbø, P. Pulay. Local configuration interaction: An efficient approach for larger molecules. *Chemical Physics Letters* **1985**, *113*, 13–18.

[61] S. Sæbø, P. Pulay. Local Treatment of Electron Correlation. *Annual Review of Physical Chemistry* **1993**, *44*, 213–236.

[62] M. Schütz, H.-J. Werner. Local perturbative triples correction (T) with linear cost scaling. *Chemical Physics Letters* **2000**, *318*, 370–378.

[63] M. Schütz. Low-order scaling local electron correlation methods. III. Linear scaling local perturbative triples correction (T). *The Journal of Chemical Physics* **2000**, *113*, 9986–10001.

[64] F. Neese, A. Hansen, D. G. Liakos. Efficient and accurate approximations to the local coupled cluster singles doubles method using a truncated pair natural orbital basis. *The Journal of Chemical Physics* **2009**, *131*, 064103.

[65] W. Li, P. Piecuch, J. R. Gour, S. Li. Local correlation calculations using standard and renormalized coupled-cluster approaches. *The Journal of Chemical Physics* **2009**, *131*, 114109.

[66] A. Hansen, D. G. Liakos, F. Neese. Efficient and accurate local single reference correlation methods for high-spin open-shell molecules using pair natural orbitals. *The Journal of Chemical Physics* **2011**, *135*, 214102.

[67] F. Neese, F. Wennmohs, A. Hansen. Efficient and accurate local approximations to coupled-electron pair approaches: An attempt to revive the

pair natural orbital method. *The Journal of Chemical Physics* **2009**, *130*, 114108.

[68] J. Yang, G. K.-L. Chan, F. R. Manby, M. Schütz, H. Werner. The orbital-specific-virtual local coupled cluster singles and doubles method. *The Journal of Chemical Physics* **2012**, *136*, 144105.

[69] M. Schütz, J. Yang, G. K.-L. Chan, F. R. Manby, H.-J. Werner. The orbital-specific virtual local triples correction: OSV-L(T). *The Journal of Chemical Physics* **2013**, *138*, 054109.

[70] Z. Rolik, M. Kállay. A general-order local coupled-cluster method based on the cluster-in-molecule approach. *The Journal of Chemical Physics* **2011**, *135*, 104111.

[71] Z. Rolik, L. Szegedy, I. Ladjánszki, B. Ladóczki, M. Kállay. An efficient linear-scaling CCSD(T) method based on local natural orbitals. *The Journal of Chemical Physics* **2013**, *139*, 094105.

[72] F. Claeyssens, J. N. Harvey, F. R. Manby, R. A. Mata, A. J. Mulholland, K. E. Ranaghan, M. Schütz, S. Thiel, W. Thiel, H.-J. Werner. High-Accuracy Computation of Reaction Barriers in Enzymes. *Angewandte Chemie International Edition* **2006**, *45*, 6856–6859.

[73] A. Anoop, W. Thiel, F. Neese. A Local Pair Natural Orbital Coupled Cluster Study of Rh Catalyzed Asymmetric Olefin Hydrogenation. *Journal of Chemical Theory and Computation* **2010**, *6*, 3137–3144.

[74] C. Riplinger, F. Neese. An efficient and near linear scaling pair natural orbital based local coupled cluster method. *The Journal of Chemical Physics* **2013**, *138*, 034106.

[75] A. Hansen, C. Bannwarth, S. Grimme, P. Petrović, C. Werlé, J.-P. Djukic. The Thermochemistry of London Dispersion-Driven Transition Metal Reactions: Getting the 'Right Answer for the Right Reason'. *ChemistryOpen* **2014**, *3*, 177–189.

[76] F. Neese, D. Liakos, S. Ye. Correlated wavefunction methods in bioinorganic chemistry. *Journal of Biological Inorganic Chemistry* **2011**, *16*, 821–829.

[77] D. Sundholm, J. Olsen. Core-valence correlation effects on the ground state electron affinity of calcium. *Chemical Physics Letters* **1994**, *217*, 451 – 455.

[78] J. Grumer, R. Zhao, T. Brage, W. Li, S. Huldt, R. Hutton, Y. Zou. Coronal lines and the importance of deep-core–valence correlation in Ag-like ions. *Physical Review A* **2014**, *89*, 062511.

[79] B. O. Roos, P. R. Taylor, P. E. Sigbahn. A complete active space SCF method (CASSCF) using a density matrix formulated super-CI approach. *Chemical Physics* **1980**, *48*, 157 – 173.

[80] J. Olsen. The CASSCF method: A perspective and commentary. *International Journal of Quantum Chemistry* **2011**, *111*, 3267–3272.

[81] K. Andersson, P. Malmqvist, B. O. Roos. Secondorder perturbation theory with a complete active space selfconsistent field reference function. *The Journal of Chemical Physics* **1992**, *96*, 1218–1226.

[82] C. Angeli, R. Cimiraglia, S. Evangelisti, T. Leininger, J.-P. Malrieu. Introduction of n-electron valence states for multireference perturbation theory. *Journal of Chemical Physics* **2001**, *114*, 10252.

[83] V. Guner, K. S. Khuong, A. G. Leach, P. S. Lee, M. D. Bartberger, K. N. Houk. A Standard Set of Pericyclic Reactions of Hydrocarbons for the Benchmarking of Computational Methods: The Performance of ab Initio, Density Functional, CASSCF, CASPT2, and CBS-QB3 Methods for the Prediction of Activation Barriers, Reaction Energetics, and Transition State Geometries. *The Journal of Physical Chemistry A* **2003**, *107*, 11445–11459.

[84] D. H. Ess, A. E. Hayden, F. Klärner, K. N. Houk. Transition States for the Dimerization of 1,3-Cyclohexadiene: A DFT, CASPT2, and CBS-QB3 Quantum Mechanical Investigation†. *Journal of Organic Chemistry* **2008**, *73*, 7586–7592.

[85] H. V. Pham, K. N. Houk. Diels–Alder Reactions of Allene with Benzene and Butadiene: Concerted, Stepwise, and Ambimodal Transition States. *The Journal of Organic Chemistry* **2014**, *79*, 8968–8976.

[86] J. A. Duncan, M. C. Spong. Ab Initio Computational Studies of Conformationally Restricted Cope Rearrangements. First Examples of Fully Concerted Allenyl Cope Rearrangements. *The Journal of Organic Chemistry* **2000**, *65*, 5720–5727.

[87] G. Tomasello, M. Garavelli, G. Orlandi. Tracking the stilbene photoisomerization in the S1 state using RASSCF. *Physical Chemistry Chemical Physics* **2013**, *15*, 19763–19773.

[88] A. Kerridge. A RASSCF study of free base, magnesium and zinc porphyrins: accuracy versus efficiency. *Physical Chemistry Chemical Physics* **2013**, *15*, 2197–2209.

[89] J. Olsen, B. O. Roos, P. Jorgensen, H. J. A. Jensen. Determinant based configuration interaction algorithms for complete and restricted configuration interaction spaces. *The Journal of Chemical Physics* **1988**, *89*, 2185–2192.

[90] P. A. Malmqvist, A. Rendell, B. O. Roos. The restricted active space self-consistent-field method, implemented with a split graph unitary group approach. *The Journal of Physical Chemistry* **1990**, *94*, 5477–5482.

[91] P. Malmqvist, K. Pierloot, A. R. M. Shahi, C. J. Cramer, L. Gagliardi. The restricted active space followed by second-order perturbation theory method: Theory and application to the study of CuO2 and Cu2O2 systems. *The Journal of Chemical Physics* **2008**, *128*, 204109.

[92] S. F. Keller, M. Reiher. Determining Factors for the Accuracy of DMRG in Chemistry. *CHIMIA International Journal for Chemistry* **2014**, *68*, 200–203.

[93] K. A. Hallberg. New trends in density matrix renormalization. *Advances in Physics* **2006**, *55*, 477–526.

[94] V. Veryazov, P. A. Malmqvist, B. O. Roos. How to select active space for multiconfigurational quantum chemistry? *International Journal of Quantum Chemistry* **2011**, *111*, 3329–3338.

[95] T. J. Lee, P. R. Taylor. A diagnostic for determining the quality of single-reference electron correlation methods. *International Journal of Quantum Chemistry* **1989**, *36*, 199–207.

[96] A. Altun, J. Breidung, F. Neese, W. Thiel. Correlated Ab Initio and Density Functional Studies on H2 Activation by FeO+. *Journal of Chemical Theory and Computation* **2014**, *10*, 3807–3820.

[97] C. L. Janssen, I. M. Nielsen. New diagnostics for coupled-cluster and Møller–Plesset perturbation theory. *Chemical Physics Letters* **1998**, *290*, 423 – 430.

[98] I. M. Nielsen, C. L. Janssen. Double-substitution-based diagnostics for coupled-cluster and Møller–Plesset perturbation theory. *Chemical Physics Letters* **1999**, *310*, 568 – 576.

[99] T. Ziegler. Approximate density functional theory as a practical tool in molecular energetics and dynamics. *Chemical Reviews* **1991**, *91*, 651–667.

[100] A. D. Becke. Perspective: Fifty years of density-functional theory in chemical physics. *The Journal of Chemical Physics* **2014**, *140*, 18A301.

[101] K. Burke. Perspective on density functional theory. *The Journal of Chemical Physics* **2012**, *136*, 150901.

[102] P. Hohenberg, W. Kohn. Inhomogeneous Electron Gas. *Physical Review* **1964**, *136*, B864–B871.

[103] W. Kohn, L. Sham. Self-Consistent Equations Including Exchange and Correlation Effects. *Physical Review* **1965**, *140*, A1133–A1138.

[104] G. Zhang, C. B. Musgrave. Comparison of DFT Methods for Molecular Orbital Eigenvalue Calculations. *The Journal of Physical Chemistry A* **2007**, *111*, 1554–1561.

[105] R. Stowasser, R. Hoffmann. What Do the KohnSham Orbitals and Eigenvalues Mean? *Journal of the American Chemical Society* **1999**, *121*, 3414–3420.

[106] R. O. Jones, O. Gunnarsson. The density functional formalism, its applications and prospects. *Reviews of Modern Physics* **1989**, *61*, 689–746.

[107] S. F. Sousa, P. A. Fernandes, M. J. Ramos. General Performance of Density Functionals. *The Journal of Physical Chemistry A* **2007**, *111*, 10439–10452.

[108] J. P. Perdew, K. Burke, M. Ernzerhof. Generalized Gradient Approximation Made Simple. *Physical Review Letters* **1996**, *77*, 3865–3868.

[109] A. D. Becke. Density-functional exchange-energy approximation with correct asymptotic behavior. *Physical Review A* **1988**, *38*, 3098–3100.

[110] J. P. Perdew. Density-functional approximation for the correlation energy of the inhomogeneous electron gas. *Physical Review B* **1986**, *33*, 8822–8824.

[111] J. Tao, J. P. Perdew, V. N. Staroverov, G. E. Scuseria. Climbing the Density Functional Ladder: Nonempirical Meta-Generalized Gradient Approximation Designed for Molecules and Solids. *Physical Review Letters* **2003**, *91*, 146401.

[112] A. D. Becke. Density-functional thermochemistry. III. The role of exact exchange. *Journal of Chemical Physics* **1993**, *98*, 5648–5652.

[113] A. D. Becke. A new mixing of Hartree–Fock and local density-functional theories. *Journal of Chemical Physics* **1993**, *98*, 1372–1377.

[114] J. P. Perdew, M. Ernzerhof, K. Burke. Rationale for mixing exact exchange with density functional approximations. *The Journal of Chemical Physics* **1996**, *105*, 9982–9985.

[115] Y. Zhao, D. G. Truhlar. Design of Density Functionals That Are Broadly Accurate for Thermochemistry, Thermochemical Kinetics, and Nonbonded Interactions. *The Journal of Physical Chemistry A* **2005**, *109*, 5656–5667.

[116] S. Grimme. Semiempirical hybrid density functional with perturbative second-order correlation. *The Journal of Chemical Physics* **2006**, *124*, 034108.

[117] F. Furche. Molecular tests of the random phase approximation to the exchange-correlation energy functional. *Physical Review B* **2001**, *64*, 195120.

[118] S. Grimme, R. Huenerbein, S. Ehrlich. On the Importance of the Dispersion Energy for the Thermodynamic Stability of Molecules. *ChemPhysChem* **2011**, *12*, 1258–1261.

[119] J. Klimeš, A. Michaelides. Perspective: Advances and challenges in treating van der Waals dispersion forces in density functional theory. *The Journal of Chemical Physics* **2012**, *137*, 120901.

[120] S. Grimme. Density functional theory with London dispersion corrections. *Wiley Interdisciplinary Reviews: Computational Molecular Science* **2011**, *1*, 211–228.

[121] S. Grimme, J. Antony, S. Ehrlich, H. Krieg. A consistent and accurate ab initio parametrization of density functional dispersion correction (DFT-D) for the 94 elements H-Pu. *The Journal of Chemical Physics* **2010**, *132*, 154104.

[122] A. Becke, E. Johnson. A density-functional model of the dispersion interaction. *Journal of Chemical Physics* **2005**, *123*, 154101.

[123] E. Johnson, A. Becke. A post-Hartree-Fock model of intermolecular interactions. *Journal of Chemical Physics* **2005**, *123*, 174104.

[124] E. Johnson, A. Becke. A post-Hartree-Fock model of intermolecular interactions: Inclusion of higher-order corrections. *Journal of Chemical Physics* **2006**, *124*, 174104.

[125] A. J. Cohen, P. Mori-Sánchez, W. Yang. Insights into Current Limitations of Density Functional Theory. *Science* **2008**, *321*, 792–794.

[126] J. Autschbach, M. Srebro. Delocalization Error and "Functional Tuning" in Kohn–Sham Calculations of Molecular Properties. *Accounts of Chemical Research* **2014**, *47*, 2592–2602, PMID: 24968277.

[127] S. Grimme, W. Hujo, B. Kirchner. Performance of dispersion-corrected density functional theory for the interactions in ionic liquids. *Physical Chemistry Chemical Physics* **2012**, *14*, 4875–4883.

[128] E. R. Johnson, M. Salamone, M. Bietti, G. A. DiLabio. Modeling Noncovalent Radical–Molecule Interactions Using Conventional Density-Functional Theory: Beware Erroneous Charge Transfer. *The Journal of Physical Chemistry A* **2013**, *117*, 947–952.

[129] A. Gansäuer, M. Seddiqzai, T. Dahmen, R. Sure, S. Grimme. Computational study of the rate constants and free energies of intramolecular radical addition to substituted anilines. *Beilstein Journal of Organic Chemistry* **2013**, *9*, 1620–1629.

[130] J. P. Perdew, K. Schmidt. Jacob's ladder of density functional approximations for the exchange-correlation energy. *AIP Conference Proceedings* **2001**, *577*, 1–20.

[131] L. Goerigk, S. Grimme. Double-hybrid density functionals. *Wiley Interdisciplinary Reviews: Computational Molecular Science* **2014**, *4*, 576–600.

[132] M. Steinmetz, S. Grimme. Benchmark Study of the Performance of Density Functional Theory for Bond Activations with (Ni,Pd)-Based Transition-Metal Catalysts. *ChemistryOpen* **2013**, *2*, 115–124.

[133] T. Weymuth, E. P. A. Couzijn, P. Chen, M. Reiher. New Benchmark Set of Transition-Metal Coordination Reactions for the Assessment of Density Functionals. *Journal of Chemical Theory and Computation* **2014**, *10*, 3092–3103.

[134] M. Swart. Spin states of (bio)inorganic systems: Successes and pitfalls. *International Journal of Quantum Chemistry* **2013**, *113*, 2–7.

[135] J. Brandenburg, S. Grimme. A dispersion-corrected density functional theory case study on ethyl acetate conformers, dimer, and molecular crystal. *Theoretical Chemistry Accounts* **2013**, *132*, 1399.

[136] S. Grimme, M. Steinmetz. Effects of London dispersion correction in density functional theory on the structures of organic molecules in the gas phase. *Physical Chemistry Chemical Physics* **2013**, *15*, 16031–16042.

[137] S. Ehrlich, J. Moellmann, S. Grimme. Dispersion-Corrected Density Functional Theory for Aromatic Interactions in Complex Systems. *Accounts of Chemical Research* **2013**, *46*, 916–926.

[138] S. Grimme. Comment on: "On the Accuracy of DFT Methods in Reproducing Ligand Substitution Energies for Transition Metal Complexes in Solution: The Role of Dispersive Interactions" by H. Jacobsen and L. Cavallo. *ChemPhysChem* **2012**, *13*, 1407–1409.

[139] W. Hujo, S. Grimme. Comparison of the performance of dispersion-corrected density functional theory for weak hydrogen bonds. *Physical Chemistry Chemical Physics* **2011**, *13*, 13942–13950.

[140] Y. Zhao, D. Truhlar. The M06 suite of density functionals for main group thermochemistry, thermochemical kinetics, noncovalent interactions, excited states, and transition elements: two new functionals and systematic testing of four M06-class functionals and 12 other functionals. *Theoretical Chemistry Accounts* **2008**, *120*, 215–241.

[141] Y. Zhao, D. G. Truhlar. Applications and validations of the Minnesota density functionals. *Chemical Physics Letters* **2011**, *502*, 1 – 13.

[142] J. P. Perdew, A. Ruzsinszky, L. A. Constantin, J. Sun, G. I. Csonka. Some Fundamental Issues in Ground-State Density Functional Theory: A Guide for the Perplexed. *Journal of Chemical Theory and Computation* **2009**, *5*, 902–908.

[143] P. Pyykkö, J. P. Desclaux. Relativity and the periodic system of elements. *Accounts of Chemical Research* **1979**, *12*, 276–281.

[144] P. Pyykkö. Theoretical chemistry of gold. *Angewandte Chemie, International Edition* **2004**, *43*, 4412–4456.

[145] H. Schmidbaur, A. Schier. Aurophilic interactions as a subject of current research: an up-date. *Chemical Society Reviews* **2012**, *41*, 370–412.

[146] M. Lein, M. Rudolph, S. K. Hashmi, P. Schwerdtfeger. Homogeneous Gold Catalysis: Mechanism and Relativistic Effects of the Addition of Water to Propyne. *Organometallics* **2010**, *29*, 2206–2210.

[147] D. J. Gorin, F. D. Toste. Relativistic effects in homogeneous gold catalysis. *Nature* **2007**, *446*, 395–403.

[148] M. Pernpointner, A. S. K. Hashmi. Fully Relativistic, Comparative Investigation of Gold and Platinum Alkyne Complexes of Relevance for the Catalysis of Nucleophilic Additions to Alkynes. *Journal of Chemical Theory and Computation* **2009**, *5*, 2717–2725.

[149] D. Andrae, U. Haussermann, M. Dolg, H. Stoll, H. Preuss. Energy-adjusted ab initio pseudopotentials for the second and third row transition elements. *Theoretica Chimica Acta* **1990**, *77*, 123–141.

[150] C. van Wüllen. Molecular density functional calculations in the regular relativistic approximation: Method, application to coinage metal diatomics, hydrides, fluorides and chlorides, and comparison with first-order relativistic calculations. *The Journal of Chemical Physics* **1998**, *109*, 392–399.

[151] D. G. Liakos, F. Neese. Interplay of correlation and relativistic effects in correlated calculations on transition-metal complexes: The $(Cu_2O_2)^{2+}$ core revisited. *Journal of Chemical Theory and Computation* **2011**, *7*, 1511–1523.

[152] J. G. Hill. Gaussian basis sets for molecular applications. *International Journal of Quantum Chemistry* **2013**, *113*, 21–34.

[153] F. Jensen. Atomic orbital basis sets. *Wiley Interdisciplinary Reviews: Computational Molecular Science* **2013**, *3*, 273–295.

[154] R. Ditchfield, W. J. Hehre, J. A. Pople. Self-Consistent Molecular-Orbital Methods. IX. An Extended GaussianType Basis for Molecular-Orbital Studies of Organic Molecules. *The Journal of Chemical Physics* **1971**, *54*, 724–728.

[155] F. Weigend, F. Furche, R. Ahlrichs. Gaussian basis sets of quadruple zeta valence quality for atoms H–Kr. *The Journal of Chemical Physics* **2003**, *119*, 12753–12762.

[156] F. Weigend, R. Ahlrichs. Balanced basis sets of split valence, triple zeta valence and quadruple zeta valence quality for H to Rn: Design and

assessment of accuracy. *Physical Chemistry Chemical Physics* **2005**, *7*, 3297–3305.

[157] F. Weigend. Accurate Coulomb-fitting basis sets for H to Rn. *Physical Chemistry Chemical Physics* **2006**, *8*, 1057–1065.

[158] D. A. Pantazis, X.-Y. Chen, C. R. Landis, F. Neese. All-electron scalar relativistic basis sets for third-row transition metal atoms. *Journal of Chemical Theory and Computation* **2008**, *4*, 908–919.

[159] D. A. Pantazis, F. Neese. All-electron scalar relativistic basis sets for the lanthanides. *Journal of Chemical Theory and Computation* **2009**, *5*, 2229–2238.

[160] D. A. Pantazis, F. Neese. All-electron scalar relativistic basis sets for the actinides. *Journal of Chemical Theory and Computation* **2011**, *7*, 677–684.

[161] D. A. Pantazis, F. Neese. All-electron scalar relativistic basis sets for the 6p elements. *Theoretical Chemistry Accounts* **2012**, *131*, 1292.

[162] D. Rappoport, F. Furche. Property-optimized Gaussian basis sets for molecular response calculations. *The Journal of Chemical Physics* **2010**, *133*, 134105.

[163] J. Zheng, X. Xu, D. Truhlar. Minimally augmented Karlsruhe basis sets. *Theoretical Chemistry Accounts* **2011**, *128*, 295–305.

[164] W. J. Hehre, R. Ditchfield, J. A. Pople. Self-Consistent Molecular Orbital Methods. XII. Further Extensions of Gaussian-Type Basis Sets for Use in Molecular Orbital Studies of Organic Molecules. *The Journal of Chemical Physics* **1972**, *56*, 2257–2261.

[165] T. Dunning Jr. Gaussian basis sets for use in correlated molecular calculations. I. The atoms boron through neon and hydrogen. *The Journal of Chemical Physics* **1989**, *90*, 1007–1023, cited By 14637.

[166] J. Tomasi, M. Persico. Molecular Interactions in Solution: An Overview of Methods Based on Continuous Distributions of the Solvent. *Chemical Reviews* **1994**, *94*, 2027–2094.

[167] C. J. Cramer, D. G. Truhlar. Implicit Solvation Models: Equilibria, Structure, Spectra, and Dynamics. *Chemical Reviews* **1999**, *99*, 2161–2200.

[168] M. Orozco, F. J. Luque. Theoretical Methods for the Description of the Solvent Effect in Biomolecular Systems. *Chemical Reviews* **2000**, *100*, 4187–4226.

[169] J. Tomasi, B. Mennucci, R. Cammi. Quantum Mechanical Continuum Solvation Models. *Chemical Reviews* **2005**, *105*, 2999–3094.

[170] A. Schäfer, A. Klamt, D. Sattel, J. C. W. Lohrenz, F. Eckert. COSMO Implementation in TURBOMOLE: Extension of an efficient quantum chemical code towards liquid systems. *Physical Chemistry Chemical Physics* **2000**, *2*, 2187–2193.

[171] A. Klamt. Conductor-like Screening Model for Real Solvents: A New Approach to the Quantitative Calculation of Solvation Phenomena. *The Journal of Physical Chemistry* **1995**, *99*, 2224–2235.

[172] A. Klamt, F. Eckert, W. Arlt. COSMO-RS: An Alternative to Simulation for Calculating Thermodynamic Properties of Liquid Mixtures. *Annual Review of Chemical and Biomolecular Engineering* **2010**, *1*, 101–122.

[173] A. Klamt. The COSMO and COSMO-RS solvation models. *Wiley Interdisciplinary Reviews: Computational Molecular Science* **2011**, *1*, 699–709.

[174] M. Renz, M. Kess, M. Diedenhofen, A. Klamt, M. Kaupp. Reliable Quantum Chemical Prediction of the Localized/Delocalized Character of Organic Mixed-Valence Radical Anions. From Continuum Solvent Models to Direct-COSMO-RS. *Journal of Chemical Theory and Computation* **2012**, *8*, 4189–4203.

[175] K. Theilacker, D. Buhrke, M. Kaupp. Validation of the Direct-COSMO-RS Solvent Model for Diels–Alder Reactions in Aqueous Solution. *Journal of Chemical Theory and Computation* **2015**, *11*, 111–121.

[176] S. Tshepelevitsh, M. Oss, A. Pung, I. Leito. Evaluating the COSMO-RS Method for Modeling Hydrogen Bonding in Solution. *ChemPhysChem* **2013**, *14*, 1909–1919.

[177] D. G. Truhlar, B. C. Garrett, S. J. Klippenstein. Current Status of Transition-State Theory. *The Journal of Physical Chemistry* **1996**, *100*, 12771–12800.

[178] J. M. Goodman, P. D. Kirby, L. O. Haustedt. Some calculations for organic chemists: boiling point variation, Boltzmann factors and the Eyring equation. *Tetrahedron Letters* **2000**, *41*, 9879 – 9882.

[179] I. M. Alecu, J. Zheng, Y. Zhao, D. G. Truhlar. Computational Thermochemistry: Scale Factor Databases and Scale Factors for Vibrational Frequencies Obtained from Electronic Model Chemistries. *Journal of Chemical Theory and Computation* **2010**, *6*, 2872–2887.

[180] R. L. Jacobsen, R. D. Johnson, K. K. Irikura, R. N. Kacker. Anharmonic Vibrational Frequency Calculations Are Not Worthwhile for Small Basis Sets. *Journal of Chemical Theory and Computation* **2013**, *9*, 951–954.

[181] P. R. Schreiner, H. P. Reisenauer, D. Ley, D. Gerbig, C.-H. Wu, W. D. Allen. Methylhydroxycarbene: Tunneling Control of a Chemical Reaction. *Science* **2011**, *332*, 1300–1303.

[182] D. Ley, D. Gerbig, P. R. Schreiner. Tunnelling control of chemical reactions - the organic chemist's perspective. *Organic and Biomolecular Chemistry* **2012**, *10*, 3781–3790.

[183] C. E. Hornsby, R. S. Paton. Natural product biosynthesis: It's all downhill from here. *Nature Chemistry* **2014**, *6*, 88–89.

[184] R. S. Mulliken. Electronic Population Analysis on LCAO–MO Molecular Wave Functions. I. *The Journal of Chemical Physics* **1955**, *23*, 1833–1840.

[185] A. E. Reed, R. B. Weinstock, F. Weinhold. Natural population analysis. *The Journal of Chemical Physics* **1985**, *83*, 735–746.

[186] E. D. Glendening, C. R. Landis, F. Weinhold. Natural bond orbital methods. *Wiley Interdisciplinary Reviews: Computational Molecular Science* **2012**, *2*, 1–42.

[187] F. Hirshfeld. Bonded-atom fragments for describing molecular charge densities. *Theoretica chimica acta* **1977**, *44*, 129–138.

[188] D. J. Shepherd, P. A. Broadwith, B. S. Dyson, R. S. Paton, J. W. Burton. Structure Reassignment of Laurefurenynes A and B by Computation and Total Synthesis. *Chemistry – A European Journal* **2013**, *19*, 12644–12648.

[189] E. V. Mercado-Marin, P. Garcia-Reynaga, S. Romminger, E. F. Pimenta, D. K. Romney, M. W. Lodewyk, D. E. Williams, R. J. Andersen, S. J. Miller, D. J. Tantillo, R. G. S. Berlinck, R. Sarpong. Total synthesis and isolation of citrinalin and cyclopiamine congeners. *Nature* **2014**, *509*, 318–324.

[190] J. C. Facelli. Calculations of chemical shieldings: Theory and applications. *Concepts in Magnetic Resonance Part A* **2004**, *20A*, 42–69.

[191] W. Kutzelnigg. Theory of Magnetic Susceptibilities and NMR Chemical Shifts in Terms of Localized Quantities. *Israel Journal of Chemistry* **1980**, *19*, 193–200.

[192] M. Schindler, W. Kutzelnigg. Theory of magnetic susceptibilities and NMR chemical shifts in terms of localized quantities. II. Application to some simple molecules. *The Journal of Chemical Physics* **1982**, *76*, 1919–1933.

[193] R. Ditchfield. Self-consistent perturbation theory of diamagnetism. *Molecular Physics* **1974**, *27*, 789–807.

[194] K. Wolinski, J. F. Hinton, P. Pulay. Efficient implementation of the gauge-independent atomic orbital method for NMR chemical shift calculations. *Journal of the American Chemical Society* **1990**, *112*, 8251–8260.

[195] G. Rauhut, S. Puyear, K. Wolinski, P. Pulay. Comparison of NMR Shieldings Calculated from Hartree-Fock and Density Functional Wave Functions Using Gauge-Including Atomic Orbitals. *The Journal of Physical Chemistry* **1996**, *100*, 6310–6316.

[196] M. W. Lodewyk, M. R. Siebert, D. J. Tantillo. Computational Prediction of 1H and 13C Chemical Shifts: A Useful Tool for Natural Product, Mechanistic, and Synthetic Organic Chemistry. *Chemical Reviews* **2012**, *112*, 1839–1862.

[197] R. Ahlrichs, M. Bär, M. Häser, H. Horn, C. Kölmel. Electronic structure calculations on workstation computers: The program system turbomole. *Chemical Physics Letters* **1989**, *162*, 165–169.

[198] F. Neese. The ORCA program system. *Wiley Interdisciplinary Reviews: Computational Molecular Science* **2012**, *2*, 73–78.

[199] O. N. Nieto Faza, R. Álvarez Rodríguez, C. Silva López. Performance of density functional theory on homogeneous gold catalysis. *Theor. Chem. Acc.* **2011**, *128*, 647–661.

[200] P. Nava, D. Hagebaum-Reignier, S. Humbel. Bonding of gold with unsaturated species. *ChemPhysChem* **2012**, *13*, 2090–2096.

[201] S. K. Hashmi, F. D. Toste (Eds.), *Modern Gold Catalyzed Synthesis*, Wiley-VCH Verlag GmbH & Co. KGaA, **2012**.

[202] N. Marion, S. P. Nolan. N-Heterocyclic carbenes in gold catalysis. *Chemical Society Reviews* **2008**, *37*, 1776–1782.

[203] A. Furstner, P. Davies. Catalytic Carbophilic Activation: Catalysis by Platinum and Gold π-Acids. *Angewandte Chemie International Edition* **2007**, *46*, 3410–3449.

[204] C. Obradors, A. M. Echavarren. Intriguing mechanistic labyrinths in gold(I) catalysis. *Chemical Communications* **2014**, *50*, 16–28.

[205] A. Furstner. From Understanding to Prediction: Gold- and Platinum-Based π-Acid Catalysis for Target Oriented Synthesis. *Accounts of Chemical Research* **2014**, *47*, 925–938.

[206] J. C. Timmerman, B. D. Robertson, R. A. Widenhoefer. Gold-Catalyzed Intermolecular Anti-Markovnikov Hydroamination of Alkylidenecyclopropanes. *Angewandte Chemie International Edition* **2014**, 2251–2254.

[207] M. S. Kharasch, H. S. Isbell. The Chemistry of organic gold compounds. III. Direct introduction of gold into the aromatic nucleus (Preliminary communication). *Journal of the American Chemical Society* **1931**, *53*, 3053–3059.

[208] W. Wang, G. B. Hammond, B. Xu. Ligand Effects and Ligand Design in Homogeneous Gold(I) Catalysis. *Journal of the American Chemical Society* **2012**, *134*, 5697–5705.

[209] M. Livendahl, C. Goehry, F. Maseras, A. M. Echavarren. Rationale for the sluggish oxidative addition of aryl halides to Au(I). *Chemical Communications* **2014**, *50*, 1533–1536.

[210] D. Wang, R. Cai, S. Sharma, J. Jirak, S. K. Thummanapelli, N. G. Akhmedov, H. Zhang, X. Liu, J. L. Petersen, X. Shi. "Silver Effect" in Gold(I) Catalysis: An Overlooked Important Factor. *Journal of the American Chemical Society* **2012**, *134*, 9012–9019.

[211] A. S. K. Hashmi, J. P. Weyrauch, M. Rudolph, E. Kurpejović. Gold Catalysis: The Benefits of N and N,O Ligands. *Angewandte Chemie International Edition* **2004**, *43*, 6545–6547.

[212] O. Seppänen, M. Muuronen, J. Helaja. Gold-Catalyzed Conversion of Aryl- and Alkyl-Substituted 1-(o-Aminophenyl)-2-propyn-1-ones to the Corresponding 2-Substituted 4-Quinolones. *European Journal of Organic Chemistry* **2014**, *2014*, 4044–4052.

[213] A. S. K. Hashmi, T. M. Frost, J. W. Bats. Highly Selective Gold-Catalyzed Arene Synthesis. *Journal of the American Chemical Society* **2000**, *122*, 11553–11554.

[214] CRC, *Handbook of Chemistry and Physics, 95th Edition*, **2014-2015**.

[215] D. Benitez, N. D. Shapiro, E. Tkatchouk, Y. Wang, W. A. Goddard, F. D. Toste. A bonding model for gold(I) carbene complexes. *Nature Chemistry* **2009**, *1*, 482–486.

[216] G. Seidel, A. Furstner. Structure of a Reactive Gold Carbenoid. *Angewandte Chemie International Edition* **2014**, *53*, 4807–4811.

[217] I. U. Khand, G. R. Knox, P. L. Pauson, W. E. Watts. A cobalt induced cleavage reaction and a new series of arenecobalt carbonyl complexes. *Journal of the Chemical Society D* **1971**, 36a.

[218] I. U. Khand, G. R. Knox, P. L. Pauson, W. E. Watts, M. I. Foreman. Organocobalt complexes. Part II. Reaction of acetylenehexacarbonyldicobalt complexes, (R1C2R2)Co2(CO)6, with norbornene and its derivatives. *Journal of the Chemical Society, Perkin Transactions 1* **1973**, 977–981.

[219] S. E. Gibson, N. Mainolfi. The Intermolecular Pauson–Khand Reaction. *Angewandte Chemie International Edition* **2005**, *44*, 3022–3037.

[220] H.-W. Lee, F.-Y. Kwong. A Decade of Advancements in Pauson–Khand-Type Reactions. *European Journal of Organic Chemistry* **2010**, *2010*, 789–811.

[221] T. J. M. de Bruin, A. Milet, A. E. Greene, Y. Gimbert. Insight into the Reactivity of Olefins in the Pauson-Khand Reaction. *The Journal of Organic Chemistry* **2004**, *69*, 1075–1080.

[222] N. Aiguabella, E. Arce, C. c. Del Pozo, X. d. Verdaguer, A. d. Riera. Pauson-Khand reaction of internal dissymmetric trifluoromethyl alkynes. Influence of the alkene on the regioselectivity. *Molecules* **2014**, *19*, 1763–1774.

[223] A. Vazquez-Romero, X. Verdaguer, A. Riera. General Approach to Prostanes B1 by Intermolecular Pausonhand Reaction: Syntheses of Methyl Esters of Prostaglandin B1 and Phytoprostanes 16-B1-PhytoP and 9-L1-PhytoP. *European Journal of Organic Chemistry* **2013**, *2013*, 1716–1725.

[224] A. Lledo, A. Fuster, M. Reves, X. Verdaguer, A. Riera. The Pauson-Khand reaction of medium sized trans-cycloalkenes. *Chemical Communications* **2013**, *49*, 3055–3057.

[225] N. Aiguabella, A. Pesquer, X. Verdaguer, A. Riera. Pauson-Khand Adducts of N-Boc-propargylamine: A New Approach to 4,5-Disubstituted Cyclopentenones. *Organic Letters* **2013**, *15*, 2696–2699.

[226] S. Orgué, T. León, A. Riera, X. Verdaguer. Asymmetric Intermolecular Cobalt-Catalyzed Pauson–Khand Reaction Using a P-Stereogenic Bisphosphane. *Organic Letters* **2015**, *17*, 250–253.

[227] P. Magnus, L. M. Principe. Origins of 1,2- and 1,3-stereoselectivity in dicobaltoctacarbonyl alkene-alkyne cyclizations for the synthesis of substituted bicyclo[3.3.0]octenones. *Tetrahedron Letters* **1985**, *26*, 4851 – 4854.

[228] M. Yamanaka, E. Nakamura. Density Functional Studies on the Pauson-Khand Reaction. *Journal of the American Chemical Society* **2001**, *123*, 1703–1708.

[229] T. J. M. de Bruin, A. Milet, F. Robert, Y. Gimbert, A. E. Greene. Theoretical Study of the Regiochemistry-Determining Step of the Pauson-Khand Reaction. *Journal of the American Chemical Society* **2001**, *123*, 7184–7185.

[230] T. J. de Bruin, C. Michel, K. Vekey, A. E. Greene, Y. Gimbert, A. Milet. First C–C bond formation in the Pauson–Khand reaction: Influence of carbon–carbon triple bond polarization on regiochemistry: A density functional theory study. *Journal of Organometallic Chemistry* **2006**, *691*, 4281 – 4288.

[231] M. E. Krafft, R. H. Romero, I. L. Scott. Pauson-Khand reaction with electron-deficient alkynes. *The Journal of Organic Chemistry* **1992**, *57*, 5277–5278.

[232] T. R. Hoye, J. A. Suriano. Dicobalt octacarbonyl-mediated cyclizations of electron-deficient alkynones. *The Journal of Organic Chemistry* **1993**, *58*, 1659–1660.

[233] F. Robert, A. Milet, Y. Gimbert, D. Konya, A. E. Greene. Regiochemistry in the Pauson-Khand Reaction: Has a Trans Effect Been Overlooked? *Journal of the American Chemical Society* **2001**, *123*, 5396–5400.

[234] J. Kizirian, N. Aiguabella, A. Pesquer, S. Fustero, P. Bello, X. Verdaguer, A. Riera. Regioselectivity in Intermolecular Pauson-Khand Reactions of Dissymmetric Fluorinated Alkynes. *Organic Letters* **2010**, *12*, 5620–5623.

[235] N. Aiguabella, C. del Pozo, X. Verdaguer, S. Fustero, A. Riera. Synthesis and Application of β-Substituted Pausonhand Adducts: Trifluoromethyl as a Removable Steering Group. *Angewandte Chemie International Edition* **2013**, *52*, 5355–5359.

[236] F. Furche, J. P. Perdew. The performance of semilocal and hybrid density functionals in 3d transition-metal chemistry. *The Journal of Chemical Physics* **2006**, *124*, 044103.

[237] K. K. Pandey, S. K. Patidar, P. Patidar, R. Vishwakarma, P. K. Bariya. Accurate Structure and Bonding Description of the Transition Metal-Disulfur Monoxide Complexes [(PMe3)2M(S2O)] (M = Ni, Pd, Pt): Grimme Dispersion Corrected DFT Study. *Zeitschrift für anorganische und allgemeine Chemie* **2014**, *640*, 370–379.

[238] J. A. Platts, G. J. S. Evans, M. P. Coogan, J. Overgaard. Electronic Structure of the Alkyne-Bridged Dicobalt Hexacarbonyl Complex Co2 μ-C2H2 (CO)6: Evidence for Singlet Diradical Character and Implications for Metal-Metal Bonding. *Inorganic Chemistry* **2007**, *46*, 6291–6298.

Appendix

I M. Muuronen, J.E. Perea-Buceta, M. Nieger, M. Patzschke and J. Helaja. *Organometallics* **2012**, *31*, 4320-4330.

IIa T. Wirtanen, M. Muuronen, M. Melchionna, M. Patzschke and J. Helaja. *Journal of Organic Chemistry* **2014**, *79*, 10269-10283.

IIb T. Wirtanen, M. Muuronen, M. Melchionna, M. Patzschke and J. Helaja. *Journal of Organic Chemistry* **2014**, *79*, 10269-10283: Pages 80-87 of the Supplementary Information.

III E. Fager-Jokela, M. Muuronen, M. Patzschke and J. Helaja. *Journal of Organic Chemistry* **2012**, *77*, 9134-9147.

IVa E. Fager-Jokela, M. Muuronen, H. Khaizourane, A. Vázquez-Romero, X. Verdaguer, A. Riera and J. Helaja. *Journal of Organic Chemistry* **2014**, *79*, 10999-11010.

IVb E. Fager-Jokela, M. Muuronen, H. Khaizourane, A. Vázquez-Romero, X. Verdaguer, A. Riera and J. Helaja. *Journal of Organic Chemistry* **2014**, *79*, 10999-11010: Pages 71-77 of the Supplementary Information.